ELAHE GHASEMIAN LANGEROUDI

QUANTITATIVE ASPECTS OF CO_2-GRAFTED AMINE INTERACTIONS IN GAS-LIQUID-SOLID SOLUBILITY EQUILIBRIUM: APPLICATION TO CO_2 CAPTURE

Mémoire présentée
à la Faculté des études supérieures de l'Université Laval
dans le cadre du programme de maîtrise en génie chimique
pour l'obtention du grade de Maîtrise ès Sciences (M.Sc.)

DÉPARTEMENT DE GÉNIE CHIMIQUE
FACULTÉ DES SCIENCES ET DE GÉNIE
UNIVERSITÉ LAVAL
QUÉBEC

2010

Résumé

Les effets liés à la présence d'eau *liquide* sur la capacité d'adsorption de CO_2 par une silice mésoporeuse de type SBA-15 fonctionnalisée au moyen des amines suivantes : aminopropyltrimethoxysilane (APS) et N-(2-aminoéthyl) -3 - (aminopropyl) trimethoxysilane (AEAPS) ont été examinés pour évaluer le potentiel de ce mode de contact dans des laveurs gaz-liquide-solide. Les résultats ont été comparés à la capacité d'adsorption de CO_2 des amines greffées dans des conditions humides et sèches ainsi qu'à la capacité d'*absorption* de CO_2 dans les systèmes gaz-liquide avec des solutions aqueuses d'amines ayant des structures semblables à celles des amines greffées. Dans ces conditions, une estimation de l'adsorption physique de CO_2 a été obtenue par l'étude de la SBA-15 non-modifiée. En outre, afin d'évaluer l'efficacité et la stabilité à long terme de l'association amine/SBA-15, les amines greffées ont été soumises à huit cycles successifs d'immersion dans les milieux aqueux d'une durée de 24 h chacune. Les échantillons récupérés ont été caractérisés au moyen de la diffraction aux rayons, des isothermes de sorption d'azote et d'analyse élémentaire CHN. Jusqu'à 40% de la quantité d'amines greffées a subi une lixiviation durant les quelques premiers cycles de régénération; par la suite, la teneur en azote de l'AEAPS est demeurée relativement stable, contrairement à l'APS qui a connu une moindre stabilité. Fait intéressant, les structures des deux matériaux greffés, APS et AEAPS, sont demeurées intactes après plusieurs expositions à l'eau. L'efficacité de capture de CO_2 la plus élevée a été obtenue dans le cas des amines aqueuses (voie homogène). Cependant, la capture de CO_2 à l'aide d'amines greffées dans le cas du système triphasique (gaz-liquide-solide) a donné lieu, pour des conditions opératoires comparables, à des valeurs intermédiaires entre les voies sèche et humide du mode de contact gaz-solide.

Abstract

The effects associated with the presence of liquid water on the CO_2 *adsorption* capacity by SBA-15 silica functionalized with aminopropyltrimethoxysilane (APS) and N-(2-aminoethyl)-3-(aminopropyl)trimethoxysilane (AEAPS) were examined to evaluate the potential of this mode of contact in gas-liquid-solid scrubbing operations for CO_2 partial pressures typical of atmospheric post-combustion flue gases. The results were compared to the CO_2 adsorption capacity of the grafted amines in moist and dry gas-solid conditions along with the CO_2 *absorption* capacity in gas-liquid amine solution systems consisting of amines with nearly identical structures. In these conditions, an estimation of CO_2 *physical* adsorption was obtained through study of (bare) unmodified SBA-15. Furthermore, to assess the efficacy and long-term stability of the amine/SBA-15 association, grafted amines were subjected to up to eight successive immersion cycle tests (24 h each) in aqueous media. The recovered samples were characterized by X-ray diffraction (XRD), nitrogen sorption isotherm and CHN elemental analysis. Up to 40% of grafted amines merely leached off in the few first regeneration cycles, thereafter the nitrogen content of AEAPS remained quite stable, unlike APS which exhibited lower stability. Interestingly, the mesoporous structures of both APS and AEAPS were preserved after several exposures to water. The highest CO_2 capture efficiency were achieved with liquid amines, while CO_2 capture using grafted amine in gas-liquid-solid systems exhibited C/N atom efficiency intermediate between those of dry and moist gas-solid systems for comparable conditions.

Foreword

A manuscript prepared from this research study was submitted to the Journal of Physical Chemistry C, while this work was submitted for evaluation:

Ghasemian Langeroudi, E.; Kleitz, F.; Iliuta, M. C.; Larachi, F. Grafted Amine/CO_2 Interactions in (Gas-) Liquid- Solid Adsorption/Absorption Equilibria. *J. Phys. Chem.C* in press, **2010** (DOI: 10.1021/jp908087e).

One chapter is prepared from the article in its integrity. However, the figures and tables were displaced from the end of research article to where they are mentioned in text. The size of the figures and tables and the size of characters inside of the figures were adjusted to fit with current manuscript format.

Prof. Faïçal Larachi is my research director and Dr. Maria Iliuta & Dr. Freddy Kleitz are my co-directors in this research study.

Acknowledgment

First and foremost, I thank Prof. Faïçal Larachi, my research director, for his support and generous help during my study and for his unique source of knowledge and way of leadership. I value very much having the opportunity to work in his research group.

I would like to express my deepest thanks to my husband, Mr. Pouya Hajiani, for his great professional help and for his unlimited support and motivation when I needed it the most.

I am deeply indebted to my parents for their infinite support and encouragements during my study.

I would also like to express my gratitude to my co-director, Dr. Freddy Kleitz. I have had the valuable opportunity to learn and be trained in his laboratory in the Chemistry department.

My deep thanks and sincere gratitude goes to my co-director Dr. Maria Iliuta. Her help and support were extremely appreciated throughout my study.

Finally, I am thankful to the technical staff of the Chemical engineering department at Laval University for their help.

Financial support from the Canada Research Chair "Green processes for cleaner and sustainable energy" and the Discovery Grants to F.L., F. K. and M. I. from the Natural Sciences and Engineering Research Council (NSERC) is gratefully acknowledged.

I dedicate this research report to my family

Table des matières

Résumé i
Abstract ii
Foreword iii
Acknowledgment iii
Table des matières vi
List of tables vii
List of figures viii
Introduction 1
I. 1 Problem definition 1
I. 2 CO_2 absorption in aqueous alkanolamine solutions 2
I. 3 CO_2 adsorption in mesoporous materials 5
I. 3. 1 A review of thermal, hydrothermal, and mechanical stabilities of some mesoporous silica 7
I. 3. 2 Surface functionalization 8
I. 3. 3 A review of CO_2 adsorption by grafted amine on silica supports 11
I. 4 Objectives 11
I. 5 literature cited 13
Chapter 1. Grafted Amine/CO_2 Interactions in (Gas-) Liquid-Solid Adsorption/Absorption Equilibria 16
1.1 Introduction 17
1.2 Experimental Methods 20
1.2.1 Chemicals 20
1.2.2 Synthesis of the SBA-15 Silica Substrate. 20
1.2.3 Preparation of the Functionalized Products. 20
1.2.4 Characterization Methods. 21
1.2.5 Hydrolytic Stability of Grafted Amine on SBA-15. 21
1.2.6 Gas-Solid Adsorption. 22
1.2.7 Gas-Liquid Absorption and Gas-Liquid-Solid Adsorption/ Absorption. 23
1.3 Results and Discussions 24
1.3.1 Characterization of Materials 24
1.3.2 Hydrothermal stability of grafted amine 26
1.3.3 Gas-Liquid Absorption & Gas-Liquid-Solid Adsorption/ Absorption. 30
1.3.4 Gas-Solid Adsorption 38
1.3.5 Adsorption Efficiency of Grafted and Non-Grafted Amine 39
1.4 Conclusions 40
1.5 Supporting Information 44
1.6 References 49
Conclusion and Recommendations 52

List of tables

Table 1. Argon and CO_2 Sweep Gases in TG/DTA.....23

Table 2. Characterization Data for Synthesized Materials..... 25

Table 3. Characterization Data for the Materials Used In Hydrothermal Stability Test 29

Table 4. Henry's law constant for CO_2 in water and comparison with literature values..... 32

Table S1. Literature Summary of Grafted Amines on Mesoporous Silica Prepared Under Different Conditions Applied for CO_2 (Gas-Solid) Adsorption..... 47

List of figures

Figure I1. Schematic representation of primary, secondary and tertiary amine..... 3

Figure I2. Schematic representation of mesoporous material..... 7

Figure I3. Schematic representation of grafted amine on mesoporous material..... 11

Figure 1. Schematic representation of the heterogeneous route, homogeneous route and gas-solid adsorption..... 19

Figure 2. A schematic representation of the GSLE setup.....24

Figure 3. Nitrogen physisorption isotherms for F-SBA-15, SBA-15, F-AEAPS and F-APS measured at -196 °C. 25

Figure 4. Hydrothermal stability test of APS and AEAPS in water..... 27

Figure 5. pH vs time profile measured at first four immersion cycles..... 28

Figure 6. Conductivity vs time profile measured at first four immersion cycles..... 28

Figure 7. Nitrogen physisorption isotherms for materials used in hydrothermal stability test. 30

Figure 8. Total captured CO_2 in solution/slurry of F-APS, AP and SBA-15 in 230 g of water versus CO_2 partial pressure. ..... .33

Figure 9. Total captured CO_2 in solution/slurry of F-AEAPS, AEAP and SBA-15 in 230 g of water versus CO_2 partial pressure..... 33

Figure 10. Equilibrium pH and conductivity in solution/slurry of (A, B): F-APS, AP and SBA-15; (C, D): F-AEAPS, AEAP and SBA-15 in 230 g of water versus CO_2 partial pressure. 35

Figure 11. Contribution of water, SBA-15, leached amine and grafted amine in total captured CO_2 of F-APS in water. 36

Figure 12. Contribution of water, SBA-15, leached amine and grafted amine in total captured CO_2 of F-AEAPS in water. 36

Figure 13. Total captured CO_2 by C4- AEAPS, AEAP and SBA-15 in 40 g of water in different CO_2 partial pressure. 38

Figure 14. Total adsorbed CO_2 by F- AEAPS, C4- AEAPS and SBA-15 in contact with humid and dry CO_2. 39

Figure 15. Adsorption efficiency of grafted and non-grafted amine in heterogeneous, homogeneous and gas- solid adsorption conditions. 40

Figure S1. A) Different types of bonding/interaction between aminopropylethoxysilane molecules and silicon oxide substrates, B) Hydrolysis of siloxane bond..... .46

Figure S2. Schematic representation of grafted amines on SBA-15 (APS and AEAPS) and their equivalent non-grafted amines (AP and AEAP) 46

Introduction

I. 1 Problem definition

Through the studies of the past five decades, global warming is believed to be caused by increased greenhouse gases (GHG) levels in the atmosphere. Among these GHG, CO_2 is the largest contributor in regard of its amount present in the atmosphere contributing to 60 percent of global warming effects.[1] Thus, many researchers have focused on ways to slow or stop global warming caused by the effects of GHG, particularly CO_2. The CO_2 level increased from 315 ppmv in 1958 to 377 and 385 ppmv in 2004 and 2009, respectively.[2,3]

There are three options to reduce total CO_2 emission into the atmosphere, for instance to reduce energy intensity, to reduce carbon intensity, and to improve the sequestration of CO_2. The first option requires efficient use of energy. The second option requires switching to use non-fossil fuels such as hydrogen and renewable energy while the third option involves the development of technologies to capture and sequester more CO_2.[4]

As a mid-term solution carbon dioxide capture and sequestration (CCS) is a good option to mitigate environmental impacts and allows using fossil energy until renewable energy technologies will become mature. Since CCS is a relatively expensive solution, it can be regarded as an insurance policy.

Power plants and other large-scale industrial processes are the main candidates for CO_2 capture. Depending on the process or power plant application, there are three main approaches for capturing CO_2, which consist of post-combustion, pre-combustion and oxyfuel combustion. In industrial processes, the CO_2 is mostly generated from a primary fossil fuel (coal, natural gas or oil), biomass, or mixtures of these fuels. All three mentioned approaches require a separation step of CO_2, H_2 or O_2 from a bulk gas stream (such as flue gas, synthesis gas, air or raw natural gas). These separation steps can be performed by means of physical or chemical solvents, membranes, solid sorbents, or by cryogenic separation.[5] The choice of a specific capture technology is mostly decided by the process conditions of plant operation.

Various researches have been either focusing on the incremental improvements of current technologies or developing new CCS approaches. Carbon dioxide capture via chemical absorption is among the commonest industrial technologies the majority of which involve the use of aqueous alkanolamine solutions.

In general, while using aqueous amines the feed gas must be free of SO_2, oxygen, and particulates, since these components react with the amine solution leading to its oxidation, degradation, and formation of heat-stable salts that ultimately result in absorbent loss and deterioration of capture efficiency. It has been reported that 1- 4 kg of MEA need to be replaced for each ton of CO_2 captured, depending on the feed gas composition and the amine concentration.[6,7] Moreover, applying CO_2 absorption processes using amine solutions in addition to its corrosive and toxic nature, consumes large amounts of energy.

Accordingly, new approaches have been proposed to overcome the limitations of the currently used liquid amine scrubbing technology. Inspired by this technology, a number of research groups developed solid-supported amine adsorbents. Following the advent of ordered mesoporous material MCM-41 in 1992,[8] there has been considerable interest in developing high-surface-area solid sorbents. Since ordered mesoporous silica has high concentrations of surface silanol groups (Si-OH), they are the mostly used for surface modification, i.e., grafting of functional groups on to the pore walls of the silica.

In the following sections, CO_2 absorption by aqueous amine and CO_2 adsorption by solid sorbent is discussed in more details.

I. 2 CO_2 absorption in aqueous alkanolamine solutions

Chemical solvent absorption is based on reactions between CO_2 and one or more basic absorbents, such as aqueous solutions of mono-, di-, or tri-ethanolamine. An advantageous characteristic of absorption is that it can be reversed by sending the CO_2-rich absorbent to a stripper where the temperature is raised. The regenerated absorbent is then returned to the absorber, creating a continuous recycling process. The disadvantages of chemical absorption processes include their limited loadings and high energy requirements resulting from the reaction stoichiometry and the heats of absorption, respectively.[9] There are also problems of corrosion and degradation.

Aqueous solutions of monoethanolamine (MEA) –[$HO(CH_2)_2NH_2$], diethanolamine (DEA) –[$HO((CH_2)_2)_2NH$] and N-methyldiethanolamine (MDEA) –[$(HO(CH_2)_2)_2NCH_3$] are widely used in industries as post-combustion CO_2 absorbent. MEA is an example of primary amine (R_1NH_2), DEA secondary amine (R_1R_2NH) and MDEA tertiary amine ($R_1R_2R_3N$), where R is an alkyl radical (Figure 1).

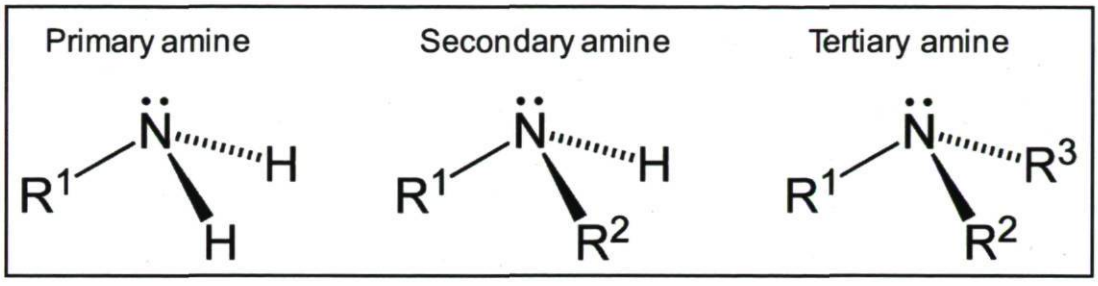

Figure 1. Schematic representation of primary, secondary and tertiary amine.

The interaction of CO_2 with primary and secondary amines in a water-free environment gives rise to the formation of carbamate and protonated amines, a reaction that requires 2 amine groups per CO_2 molecule (i.e., CO_2/N =0.5). Several reaction mechanisms are proposed in literature [10, 11, 12]. The *zwitterion* mechanism is one of the most widely accepted mechanisms for primary and secondary amines reactions with CO_2 [13] which is presented below:

For primary amines:

$$CO_2 + R_1NH_2 \leftrightarrow R_1NHCOOH \quad (1)$$

$$R_1NHCOOH + R_1NH_2 \leftrightarrow R_1NHCOO^- + R_1NH_3^+ \quad (2)$$

For secondary amines:

$$CO_2 + R_1R_2NH \leftrightarrow R_1R_2NCOOH \quad (3)$$

$$R_1R_2NCOOH + R_1R_2NH \leftrightarrow R_1R_2NCOO^- + R_1R_2NH_2^+ \quad (4)$$

Where the global reaction between CO_2 and primary and secondary amines is as follows:

For primary amines:

$$CO_2 + 2R_1NH_2 \leftrightarrow R_1NHCOO^- + R_1NH_3^+ \quad (5)$$

For secondary amines:

$$CO_2 + 2R_1R_2NH \leftrightarrow R_1R_2NCOO^- + R_1R_2NH_2^+ \quad (6)$$

On the other hand, when water is present or at higher partial pressure of CO_2, a low carbamates hydrolysis occurs. The carbamates hydrolysis forms bicarbonate and generates free amine that can react with additional CO_2. The carbamates hydrolysis is represented by the following reactions: [10-13]

For primary amines:

$$R_1NHCOO^- + H_2O \leftrightarrow HCO_3^- + R_1NH_2 \quad (7)$$

For secondary amines:

$$R_1R_2NCOO^- + H_2O \leftrightarrow HCO_3^- + R_1R_2NH \quad (8)$$

At elevated pH (>10), bicarbonate ion (HCO_3^-) forms carbonate (CO_3^{2-}) by the following reaction:

For primary amines:

$$HCO_3^- + R_1NH_2 \leftrightarrow R_1NH_3^+ + CO_3^{2-} \quad (9)$$

For secondary amines:

$$HCO_3^- + R_1R_2NH \leftrightarrow R_1R_2NH_2^+ + CO_3^{2-} \quad (10)$$

The carbamates formation is not exclusive of environments where water is absent. It is found that the production of carbamate is much faster than the formation of bicarbonate. [14] In fact, carbamate formation is not a reaction intermediate in the generation of bicarbonate,

the two probable reaction pathways between amines and CO_2 are competitive reactions with kinetics favoring the formation of carbamates.[15] For instance, the production of bicarbonate is only reported when a long contact time is allowed.[16] It was proposed that the formation of bicarbonate without the intermediacy of carbamate occurs after the first reaction pathway has produced enormous amounts of carbamate, then the equilibrium favors the reverse reaction that regenerate CO_2. Accordingly, in dry environments it would represent a macroscopic equilibrium, while in presence of water, the recovered CO_2 would have the potential to produce bicarbonate.[16, 17]

On the other hand, there is a class of amines labelled tertiary amines that possess no hydrogen atom attached to the nitrogen, as in the case of primary and secondary amines. Thus, the carbamation reaction cannot occur, resulting in a low reactivity with respect to CO_2. Instead, tertiary amines facilitate the CO_2 hydrolysis reaction forming bicarbonates. Therefore, the CO_2 loading capacity of tertiary amines is 1 mol of CO_2 per 1 mol of amine. The reaction heat released in bicarbonate formation is lower than that of carbamate formation, thus reducing solvent regeneration costs. [18] The CO_2 absorption rates of tertiary amines can be enhanced by the addition of small amounts of primary or secondary amines.

Another class of amines called sterically hindered amines, with regeneration costs lower than those of conventional primary and secondary amines. A sterically hindered amine is a primary amine in which the amino group is attached to a tertiary carbon atom, or a secondary amine in which the amino group is attached to a secondary or tertiary carbon atom. [19] 2-Amino-2-methyl-1- propanol (AMP) and 2-piperidineethanol (PE) are examples of sterically hindered primary and secondary amines, respectively. Due to the bulkiness of carbon groups attached to the nitrogen atom, these amines form unstable carbamates, which lead to carbamates hydrolysis. As mentioned before, through carbamates hydrolysis bicarbonate forms and a free amine generate. Consequently, CO_2 capacity of sterically hindered amine is 1 mol of CO_2 per 1 mol of amine. [19, 20]

I. 3 CO_2 adsorption in mesoporous materials

To remedy the problems of using aqueous amine, recent researches were focused on gas-solid adsorption as an alternative separation technique. Various zeolitic and non zeolitic

adsorbents have been examined,[21] however, many of the adsorbents developed thus far suffer from problems such as low capacity, poor selectivity, poor tolerance to water, and high-temperature regeneration or activation. Following the advent of ordered mesoporous material MCM-41 in 1992,[8] different mesoporous materials have been synthesized (e.g., HMS,[22] PCH,[23] SBA [24] and MSU. [25]

MCM-41, which was first synthesized in 1992, had a uniform hexagonal array of pores with the size range of 1.5 - 10 nanometres. This material was named Mobil Crystalline Materials, or MCM-41.[8]

In 1996, KIT-1 (Korea AdvancedInstitute of Science and Technology Number 1), was synthesized by an electrostatic templating route using sodium silicate, HTAC1, and ethylenediaminetetraacetic acid tetrasodium salt (EDTANa4).[26]

Six years later the advent of ordered mesoporous material MCM-41, researchers at the University of California in Santa Barbara announced that they had produced silica nanoparticles with larger pores of 4.6 to 30 nanometre. [24] The material was named Santa Barbara Amorphous type material, or SBA-15. These particles also have a hexagonal array of pores.

Mesoporous silica nanoparticles are generally synthesized by reacting silica precursor with a template. The result is a collection of nano-sized spheres or micron-sized amorphous powder that are filled with a regular arrangement of pores. The template can then be removed by washing with a solvent adjusted to the proper pH or via ethanol extraction or calcinations. In mesoporous material, the presence of large and tunable uniform pores in the nanometer range were found to be particularly attractive as adsorbents and supports (figure 2).

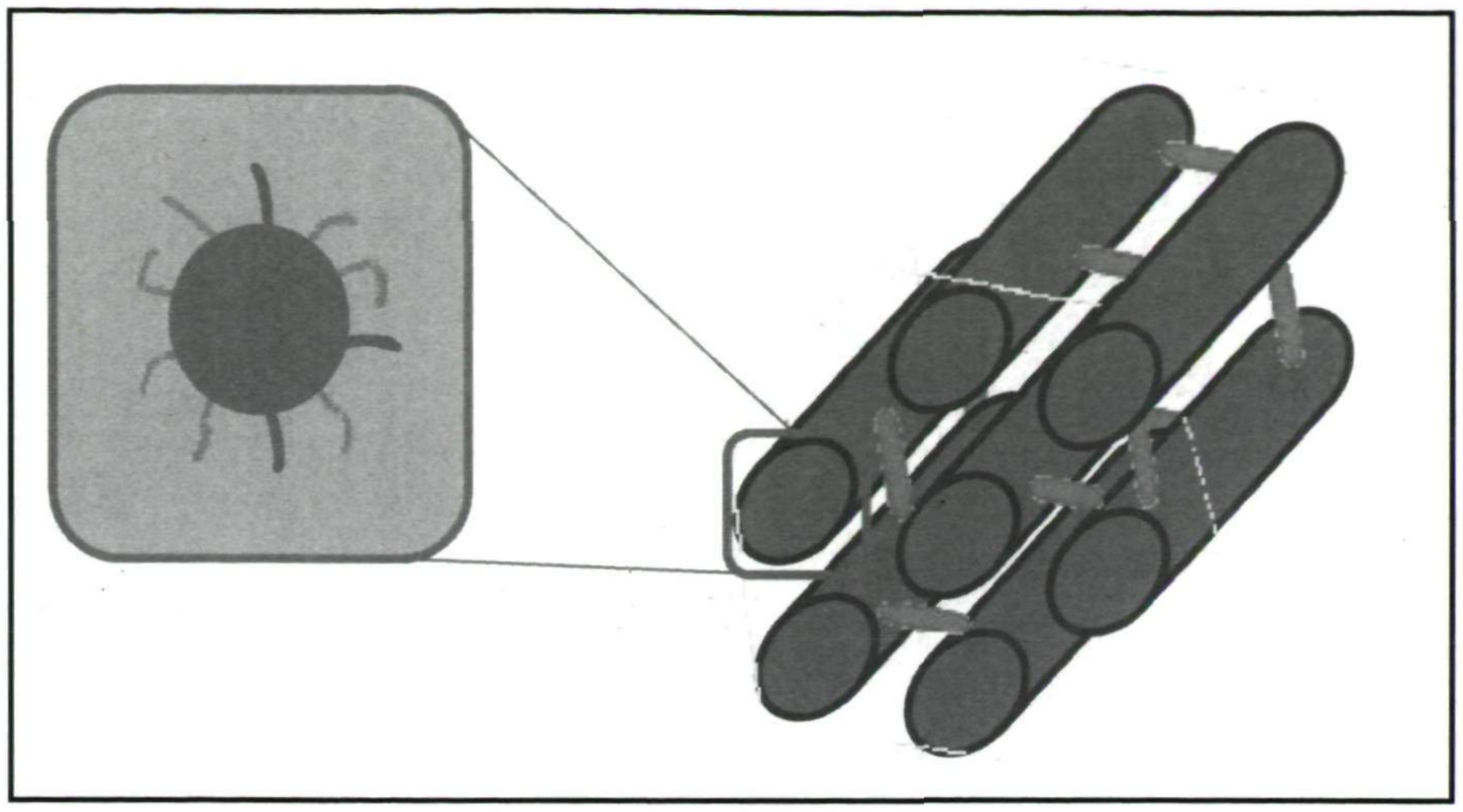

Figure 2. Schematic representation of mesoporous material

I. 3. 1 A review of thermal, hydrothermal, and mechanical stabilities of some mesoporous silica

It is recognized that the thermal, hydrothermal, and mechanical stabilities are crucial parameters for large-scale industrial applications of mesoporous material. A study by Cassiers, et al [27] revealed that:

- The thermal stability is strongly related to the wall thickness and the silica precursor used during synthesis.

SBA-15, which is prepared by TEOS (silica precursor), showed a much higher thermal stability than the other tested hexagonal TEOS-made mesostructures. One should note that the wall thickness of SBA-15 is almost three times larger (29.7 Å) than those of HMS (10.7 Å) and MCM-41(T) (9.7 Å).

- The hydrothermal stability is influenced by the wall thickness and the polymerization degree; the silica source does not play a significant role in the hydrothermal stability.

Hexagonal mesostructures with similar wall thicknesses have been compared. Consequently, the following stability trend was reported: [27] KIT-1 (colloid silica), MCM-41 (fumed silica) > FSM16 (layered silicate) > MCM-41 (TEOS), HMS (TEOS). Moreover,

SBA- 15 shows a much higher thermal stability than HMS and MCM-41 synthesized with TEOS that might be attributed to its 3-times-thicker pore walls.

- The mechanical stability is little influenced by the nature of the mesoporous molecular sieves.

The results show that all mesoporous materials collapsed at a maximum pelletizing pressure of 450 MPa. Furthermore, at a compression of 296 MPa, FSM-16 and MCM- 48 are more fragile than the other samples.

According to Cassiers et al., [27] although none of the mesoporous materials shows high mechanical stability, SBA-15, prepared with TEOS, outperforms other hexagonal mesostructures in terms of thermal/hydrothermal stability.

I. 3. 2 Surface functionalization

Mesoporous silica with large pore size has potential concerns in many areas, since the variety of molecules with different molecular sizes, can be accommodated by the pores. In addition, a high concentration of surface Si–OH groups [28] has been noted as a strong point for binding guest molecules and surface modifications.

Pure silica surfaces do not interact very strongly with carbon dioxide because the surface hydroxyl groups are not able to make strong enough interactions. Therefore, the modification of the surface by adding functional groups is an appealing means to modify surface properties and to increase the gas-adsorbent interactions. Thus, the combination of mesoporous materials and amine functional groups enable the researchers to profit from strong interactions between the carbon dioxide molecules and the amine groups as well as the good accessibility of the porous material.

The idea of functionalizing mesoporous material with amine group, for CO_2 adsorption purposes has been examined by many groups.[29- 31]

Two commonly applied methods for the introduction of functional groups onto the silica surface are co-condensation or One-Pot Synthesis (OPS) [32, 33] and post-synthesis or post-grafting. [34]

There are large differences between the availability of the amine function for materials functionalized by different methods and the differences calculated, as the number of accessible amine groups per unit area can be 20-fold.[35]

In one-pot synthesis SBA-15 formation and functionalization takes place at the same time, while in post-grafting, the functionalization is accomplished after the synthesis of SBA-15. Both methods have certain drawbacks.

In one-pot synthesis, mesostructured is prepared by silica phases via co-condensation of tetraalkoxysilanes with organosilanes in the presence of structure-directing agents leading to materials with organic residues anchored covalently to the pore walls. By using structure-directing agents known from the synthesis of pure mesoporous silica phases (e.g., MCM or SBA silica phases), organically modified silicas can be prepared in such a way that the organic functionalities project into the pores. [36]

Hoffmann et al. [36] categorized advantages and disadvantages of OPS process as listed below:

Advantages:

1) Pore blocking does not occur in OPS method since the organosilanes are direct components of the silica matrix.

2) The organic units are more homogeneously distributed than in materials synthesized with the grafting process.

Disadvantages:

1) The degree of mesoscopic order of the products decreases with increasing concentration of organosilanes in the reaction mixture, which might lead to disordered products.

2) The proportion of terminal organic groups that are incorporated into the pore-wall network is lower than which would correspond to the starting concentration of the reaction mixture.

3) Care must be taken to avoid destroying the organic functionality during removal of the surfactant. This is why in most cases, only extractive methods can be used, and calcinations are usually unsuitable.

On the other hand, post-grafting process is carried out primarily by reaction of organosilanes with the silanol groups on synthesized mesoporous silica. A schematic representation of grafted amine on mesoporous material is shown in figure 3. The silanization is generally conducted in organic solvents (i.e. toluene). It has been reported that the presence of physisorbed water on the silica surface has an effect on functionalization.[37, 38] Some studies recommend that surface water is crucial for the silanization reaction,[39] while others report that the silanization reaction can occur even in the absence of water [29, 30]. In water-free conditions, the number of surface hydroxyl groups and their accessibility play the main role in concentration and distribution of organic moieties.[40] The advantage of post-grafting is that, under the synthetic conditions used, the mesostructure skeleton of the substrate is usually retained, although it is reasonable to expect some changes in pore volume and pore diameter depending upon the size of the organic residue and the degree of occupation.[36] The post-grafting method typically results in inhomogeneous surface coverage due to congregating of organic moieties close to the entries of the mesopores and the exterior surfaces.[40] If the organosilanes react at the pore windows during the initial stages of the grafting process, further molecules can hardly enter into the center of the pores that cause a inhomogeneous distribution of the organic groups which in extreme cases can lead to complete blocking of the pores. Pore blocking occurs more in silica with small pores rather than those with large pores and can be detected by characterization methods during desorption of nitrogen from a mesoporous material at 77 K.[41]

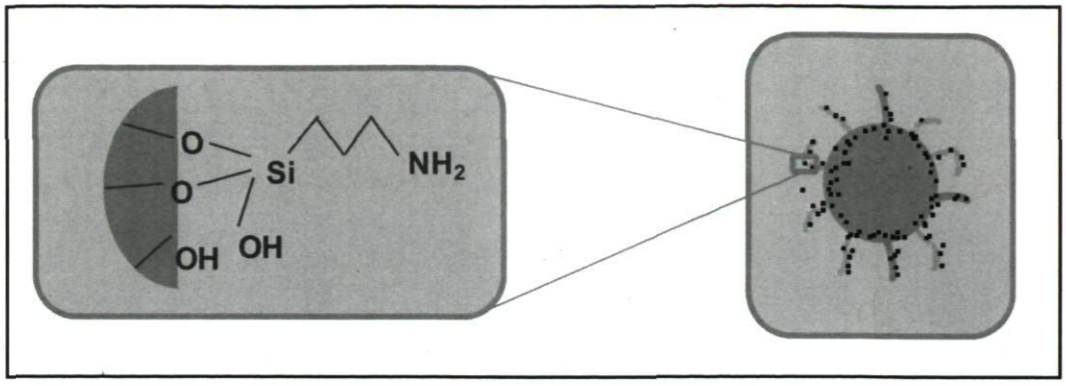

Figure 3. Schematic representation of grafted amine on mesoporous material

I. 3. 3 A review of CO_2 adsorption by grafted amine on silica supports

A review of the literature concerning amine grafting on silica based supports under dry and humid condition with the goal of enhanced CO_2 adsorption is available in Table S1 (see page 47). It can show that CO_2 adsorption capacity and C/N efficiency may respond differently whether moist is present or not in the CO_2-ladden gas streams. Such sensitivity is affected by the prevailing CO_2 feed partial pressure, temperature and amine loading, and to some extent, by the structure of sorbent. In several cases, CO_2 adsorption capacity and C/N efficiency in presence of moisture outperform their counterparts in dry conditions. Except for one reported case,[42] moisture was found indolent, particularly at the highest tested adsorption temperatures. Hence, one can conclude that in most cases, CO_2 adsorption capacity is enhanced or, at worst, remains insensitive in presence of water vapor.

I. 4 Objectives

The aim of this work is to study the effect of *liquid*-state water on CO_2 adsorption capacity of grafted amines on mesoporous materials. SBA-15 is retained as a support in our study as it is reported to outperform other hexagonal TEOS-triggered mesostructures in terms of thermal and hydrothermal stability. [27] To afford CO_2-specific adsorbents, mono-and di-amine moieties were grafted on SBA-15.

The objectives of this research are: (i) to determine the efficacy of amine/SBA-15 association sorbent in presence of liquid water, (ii) to study the effect of liquid water on CO_2 adsorption capacity of amines grafted on SBA-15 (gas-liquid-solid adsorption/absorption heterogeneous route), (iii) to measure the CO_2 absorption capacity of

(nearly-identical-structure) amines in aqueous solutions (homogeneous route), (iv) to determine, for comparative purposes, the adsorption capacity of amines grafted on SBA-15 in contact with dry and humid CO_2 (gas-solid adsorption route), and (v) to compare the results obtained in steps (i)- (iv).

Heterogeneous, homogeneous and gas- solid adsorption experiments were conducted at 30°C over CO_2 partial pressure ranging from 15 to 105 kPa. Detailed information about the process of experiment is provided in the next chapter.

I. 5 literature cited

(1) Yamasaki, A. *J. Chem. Eng. Jpn.* **2003**, *36* (4), 361-375.

(2) Monastersky, R. *Nature* **2009**, *458* (7242), 1091-1094.

(3) Hofmann, D. J.; Butler, J. H.; Tans, P. P. *Atmos. Environ.* **2009**, *43*, 2084–2086.

(4) Pennline, H. W.; Luebke, D. R.; Jones, K. L.; Myers, C. R.; Morsi, B. I.; Heintz, Y. J.; Ilconich, J. B. *Fuel Process. Technol.* **2008**, *89* (9), 897-907.

(5) Metz, B.; Davidson, O.; Coninck, H.; Loos, M.; Meyer, L. *IPCC Special Report on Carbon Dioxide Capture and Storage* **2005**. New York, United Kingdom and New York: Cambridge University Press.

(6) Chi, S.; Rochelle, G. T. *Ind. Eng. Chem. Res.* **2002**, *41* (17), 4178-4186.

(7) Strazisar, B. R.; Anderson, R. R.; White, C. M. *Abstracts of Papers of the American Chemical Society* **2002**, *223*, U569-U569.

(8) Kresge, C. T.; Leonowicz, M. E.; Roth, W. J.; Vartuli, J. C.; Beck, J. S. *Nature* **1992**, *359* (6397), 710 -712.

(9) Ma'mun, S.; Svendsen, H. F.; Hoff, K. A.; Juliussen, O. *Energy Convers. Manage.* **2007**, *48* (1), 251-258.

(10) Danckwerts, P. V. *Chem. Eng. Sci.* **1979**, *34* (4), 443-446.

(11) Al-Juaied, M., & Rochelle, G. T. *Ind. Eng. Chem. Res.***2006**, *45* (8), 2473–2482.

(12) Arstad, B.; Blom, R.; Swang, O. *J. Phys. Chem.. A* **2007**, *111* (7), 1222 -1228.

(13) Versteeg, G. F.; Van Dijck, L. A.; Van Swaaij, W. P. *Chem. Eng. Commun.* **1996**, *144* (1), 113 - 158.

(14) Vaidya, P. D.; Kenig, E. Y. CO_2-alkanolamine reaction kinetics: *Chem. Eng. Technol.* **2007**, *30* (11), 1467 -1474.

(15) Serna-Guerrero, R.; Da'na, E.; Sayari, A. *Ind. Eng. Chem. Res.***2008**, *47* (23), 9406–9412.

(16) Bottinger, W.; Maiwald, M.; Hasse, H. *Fluid Phase Equilib.* **2008**, *263*, 131–143.

(17) Da Silva, E.; Svendsen, H. *Int. J. Greenhouse Gas Control* **2007**, *1* (2), 151-157.

(18) Skinner, F. D.; Kosch, J.; Gamez, J. P. *Oil Gas J.* **1996**, *94* (11), 76-79.

(19) Sartori, G.; Savage, D. W. *Ind. Eng. Chem. Fundam.* **1983**, *22* (2), 239–249.

(20) Tontiwachwuthikul, P.; Meisen, A.; Jim Lim, C. *J. Chem. Eng. Data* **1991**, *36* (1), 130-133.

(21) Harlick, P. E.; Sayari, A. *Ind. Eng. Chem. Res.* **2007**, *46*, 446-458.

(22) Tanev, P. T.; Pinnavaia, T. J. *Science* **1995**, *267* (5199), 865 -867.

(23) Galarneau, A.; Barodowalla, A.; Pinnavaia, T. J. *Nature* **1995**, *374* (6522), 529 -531.

(24) Zhao, D.; Feng, J.; Huo, Q; Melosh, N.; Fredrickson, G. H.; Chmelka, B. F. ; Stucky, G. D. *Science* **1998**, *279* (5350), 548-552.

(25) Bagshaw, S. A.; Prouzet, E.; Pinnavaia, T. J. *Science* **1995**, *269* (5228), 1242-1244.

(26) Ryoo R.; Kim J. M.; Ko C. H.; Shin C. H. *J. Phys. Chem.* **1996**, 100 (45), 17718-17721

(27) Cassiers, K.; Linssen, T.; Mathieu, M.; Benjelloun, M.; Schrijnemakers, K., Van Der Voort, P.; Cool, P.; Vansant, E. F. *Chem. Mater.* **2002**, *14* (5), 2317-2324.

(28) Zhao, X. S.; Lu, G. Q. *J. Phys. Chem. B* **1998**, *102*, 1556–1561.

(29) Hiyoshi, N.; Yogo, K.; Yashima, T. *Microporous Mesoporous Mater.* **2005**, *84*, 357–365.

(30) Knowles, G. P.; Graham, J. V.; Delaney, S. W.; Chaffee, A. L. *Fuel Process. Technol.* **2005**, *86* (14-15), 1435-1448.

(31) Huang, H. Y.; Yang, R. T.; Chinn, D.; Munson, C. L. *Ind. Eng. Chem. Res.* **2003**, *42* (12), 2427 -2433.

(32) Yang, C. M.; Zibrowius, B.; Schüth, F. ; *Chem. Commun.* **2003**, 1772 - 1773.

(33) Mbaraka, I. K.; Shanks, B. H. *J. Catal.* **2005**, *229*, 365–373.

(34) Chang, A.; Chuang, S. S.; Gray, M.; Soong, Y. *Energy Fuels* **2003**, *17* (2), 468–473.

(35) Hoffmann, F.; Cornelius, M.; Morell, J.; Froba, M. *Angew. Chem. Int. Ed.* **2006**, *45*, 3216 – 3251.

(36) Rosenholm J. M. ; Linden M. *Chem. Mater.* **2007,** 19, 5023-5034

(37) Wasserman, S. R.; Tao, Y. T.; Whitesides, G. M. *Langmuir* **1989**, *5* (4), 1074-1087.

(38) Silberzan, P.; Leger, L.; Ausserre, D.; Benattar, J. J. Silanation of silica surfaces. *Langmuir* **1991**, *7* (8), 1647–1651.

(39) Simon, A.; Cohen-Bouhacina, T.; Porté, M. C.; Aimé, J. P.; Baquey, C. *J. Colloid Interface Sci.* **2002**, *251* (2), 278-283.

(40) Lim, M. H.; Stein, A. *Chem. Mater.* **1999**, *11* (11), 3285–3295.

(41) Rigby, S. P.; Fletcher, R. S. *J. Phys. Chem. B* **2004**, *108* (15), 4690-4695.

(42) Knowles, G. P.; Delaney, S. W.; Chaffee, A. L. *Nanoporous Materials - IV* **2005**, *156*, 887-896.

Chapter 1. Grafted Amine/CO_2 Interactions in (Gas-) Liquid-Solid Adsorption/Absorption Equilibria

Elahe Ghasemian Langeroudi,[a] Freddy Kleitz,[b] Maria.C. Iliuta,[a] Faïçal Larachi[a1]

[a]Department of Chemical Engineering; 1065, Avenue de la Médecine, Québec, QC, G1V 0A6, Canada

[b]Department of Chemistry, Laval University, 1045, Avenue de la Médecine, Québec, QC, G1V 0A6, Canada

Abstract. The effects associated with the presence of liquid water on the CO_2 *adsorption* capacity by SBA-15 silica functionalized with aminopropyltrimethoxysilane (APS) and *N*-(2-aminoethyl)-3-(aminopropyl)trimethoxysilane (AEAPS) were examined to evaluate the potential of this mode of contact in gas-liquid-solid scrubbing operations for CO_2 partial pressures typical of atmospheric postcombustion flue gases. The results were compared to the CO_2 adsorption capacity of the grafted amines in moist and dry gas-solid conditions along with the CO_2 *absorption* capacity in gas-liquid amine solution systems consisting of amines with almost identical structures. In these conditions, an estimation of CO_2 *physical* adsorption was obtained through study of (bare) unmodified SBA-15. Furthermore, to assess the efficacy and long-term stability of the amine/SBA-15 association, grafted amines were subjected to up to eight successive immersion cycle tests (24 h each) in aqueous media. The recovered samples were characterized by X-ray diffraction (XRD), nitrogen sorption isotherm, and CHN elemental analysis. Up to 40% of grafted amines merely leached off in the first few regeneration cycles; thereafter, the nitrogen content of AEAPS remained quite stable, unlike APS which exhibited lower stability. Interestingly, the mesoporous structures of both APS and AEAPS were preserved after several exposures to water. The highest CO_2 capture efficiency was achieved with liquid amines, while CO_2 capture efficiency using grafted amines in gas-liquid-solid systems was intermediate between the ones in dry and in moist gas-solid systems for comparable conditions.

[1] Corresponding author: Tel.: +1 (418) 656-3566, Fax: +1 (418) 656-5993, Faical.Larachi@gch.ulaval.ca

1.1 Introduction

Links of global warming to increased levels of greenhouse gases (GHG) in the atmosphere are anticipated to require drastic mitigation actions.[1] Carbon dioxide is the largest GHG contributor with regard to an estimated yearly release in the atmosphere of ca. 9 billion tons so estimated to contribute for ca. 60% of the global warming effects.[2,3] The CO_2 level increased from 315 ppmv in 1958 to 377 and 385 ppmv in 2004 and 2009, respectively.[3,4] Current research focuses on upstream measures to slow down CO_2 emissions into the atmosphere via reductions in energy and/or carbon intensities or, alternatively, on downstream ways to enhance CO_2 capture and sequestration (CCS). Relying on fossil energy until proven renewable energy technologies will become available requires deploying efficient CCS technologies as downstream mitigation measures.[5] Carbon dioxide capture via chemical absorption is among the most common industrial technologies, the majority of which involves the use of aqueous alkanolamine solutions. Because of their link to corrosion, stability, and degradation issues, aqueous amines in their use require several energy- and cost-penalizing preparation steps. For instance, the gas effluents to be treated must be SOx-free and eventually O2-depleted, as these constituents are known to react with amines, leading to their oxidation and/or degradation and/or formation of parasitic heat-stable salts occasioning absorbent loss. This will supply of costly makeup as well as drop in capture and energy efficiencies. It has been reported that up to 4 kg of monoethanolamine (MEA) could be off-track for each ton of CO_2 captured.[6,7]

To give perspective to numbers, this would translate into ca. 5 × 103 kg/day MEA replacement rate in 400 MW integrated gasification with combined cycle (IGCC). As an example, heat production from Athabasca coke bitumen gasification would enable therefrom daily extraction of ca. 38 000 bitumen barrels from steam assisted gravity drainage technology, should bitumen coke be used as an energy-source alternative instead of current naturalgas bitumen extraction.[8] To solve such problems associated with using aqueous amines, alternate research paths focus on more economical separation techniques relying on amine-functionalized supports. Gas-solid adsorption over amine-grafted or amine-impregnated materials is one such path where screening of a large body of CO_2-dedicated sorbents has become available in the patent and academic literature. A comprehensive account on the gas-solid amine-mediated CO_2 removal has been recently provided by Sayari and co-workers.[9,10]

Ordered mesoporous silica material supports exhibiting high surface area, high pore volume, and large pore sizes are being increasingly explored for potential use as sorbents, functionalized with amine moieties for CO_2 capture in *gas-solid* adsorption applications.[9-17] Integration of covalently linked functional amine moieties in such materials is usually achieved owing to the presence of surface Si-OH

groups, procurable in high concentrations, and easily accessible in the high surface area porous supports.[18,19] The sorbent fitting-out with amines must provide functional materials with sufficient surface area but also with pore size and pore volume compatible with CO_2 and H_2O van der Waals molecular diameters. To help stand to sense CO_2 and H_2O pore transit/crossover during carbonation/ carbamation, these diameters are, respectively, 0.47 nm[20] and 0.282 nm.[21]

A synthetic summary on the support characteristics, grafting conditions, and ensuing amine loadings, CO_2 feed partial pressures, CO_2 adsorption capacities (in mmol of CO_2/g of support), and C/N efficiencies (mol of C/mol of N) reported in some recent studies is provided in Table S1 of the Supporting Information. One remarkable observation to emerge thereof is that none has performed CO_2 adsorption in a pool of *liquid* state water surrounding the sorbents such as in liquid-solid or in (gas-) liquid-solid contacting conditions. Another observation from Table S1 is that CO_2 adsorption capacity and C/N efficiency may respond differently whether moisture is present or not in the CO_2-ladden gas streams. Such sensitivity is affected by the CO_2 feed partial pressure, temperature, amine loading, and, to some extent, the support-molecule interactions. In several cases, CO_2 adsorption capacity and C/N efficiency in the presence of moisture outperform their counterparts in dry conditions. Except for one reported case,[14] moisture was found indolent, particularly at the highest tested adsorption temperatures. Hence, one can conclude that, in most cases, CO_2 adsorption capacity is enhanced or, at worst, remains insensitive in the presence of water vapor.

There seems to be reasonable indications that the CO_2-amine reactions share commonalities in homogeneous and heterogeneous systems.[12] The basic understanding garnered from the homogeneous chemistry can serve as a starting point for interpreting CO_2-amine reactions within nanometric fluid-solid enclosures such as those stemming inside mesoporous structures. [10] One such basic analogy is that CO_2 interacts with amines according to two parallel and competitive paths: (i) a water-indifferent carbamate-forming route which involves two amine nitrogen atoms per CO_2 molecule for hydrogen-bearing nitrogen atoms as in primary or secondary amines; (ii) an amine-catalyzed water-mediated bicarbonate-forming CO_2 hydration. Path ii is stoichiometrically more interesting than path i because it yields a C/N efficiency of unity instead of the 0.5 value of path i. Making allowance of thermodynamic feasibility solely, one expects the net C/N efficiency to be a weighted average between path i and ii contributions, along with, if any, nonspecific physisorption as well. Depending on the stability of carbamates and bicarbonate, and carbamate-bicarbonate interconversion, the C/N efficiency would trail in between these two limits. These observations incited us to study the effect of *liquid*-state water on

CO_2 adsorption capacity in the presence of amines grafted on mesoporous materials. Though likening conventional gas-liquid amine (nonporous) packing bed scrubbing with the difference here that amines are immobilized on a fixed-bed scrubber with porous particles, it seems this latter contacting mode has thus far been overlooked in the literature studies. Because gas-liquid absorption and liquid-solid adsorption phenomena are the dominant mechanisms in this context, inference of CO_2 adsorption capacity on the basis of behavior of grafted amines in moist and dry gas-solid adsorption conditions would be mere conjecture and needs verification. SBA-15 is retained as a support in our study, as it is reported to outperform other hexagonal TEOS-triggered mesostructures in terms of thermal and hydrothermal stability.[22]To afford CO_2- specific adsorbents, mono and diamine moieties were grafted on SBA-15 adapted from standard procedures.[16]

The objectives of this research are: (i) to determine the efficacy of amine/SBA-15 association as a sorbent in the presence of liquid water, (ii) to study the effect of liquid water on CO_2 adsorption capacity of amines grafted on SBA-15 (gas-liquid-solid adsorption/absorption heterogeneous route), (iii) to measure the CO_2 absorption capacity of (identicalstructure) amines in aqueous solutions (homogeneous route), (iv) to determine, for comparative purposes, the adsorption capacity of amines grafted on SBA-15 in contact with dry and humid CO_2 (gas-solid adsorption route), and (v) to compare the results obtained in steps i-iv. Figure 4 displays a schematic representation of the different heterogeneous and homogeneous routes.

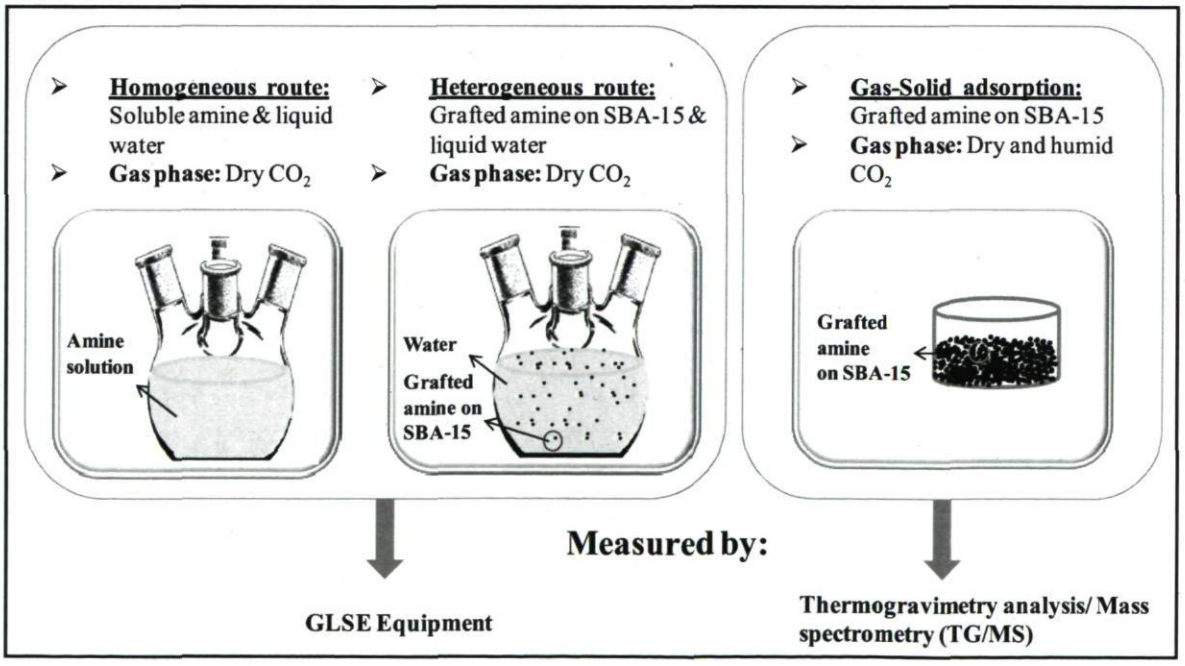

Figure 4. Schematic representation of the heterogeneous route, homogeneous route and gas-solid adsorption

1.2 Experimental Methods

1.2.1 Chemicals

Pluronic P123 ($EO_{20}PO_{70}EO_{20}$, poly(ethylene glycol)-block-poly(propylene glycol)-block-poly(ethylene glycol)), TEOS (tetraethyl orthosilicate, 98%), HCl (12 M, 37,25%), 3-(aminopropyl)trimethoxysilane ($H_2NCH_2CH_2CH_2Si(OCH_3)_3$, abbreviated as APTMS, ≥99%), 2-propylaminoethylamine ($CH_3CH_2CH_2NHCH_2CH_2NH_2$, abbreviated as AEAP, ≥97%), and 1-aminopropane ($CH_3CH_2CH_2NH_2$, abbreviated as AP, ≥99%) were purchased from Aldrich Chemical Co., and *N*-(2- aminoethyl)-3-(aminopropyl) trimethoxysilane ($H_2NCH_2CH_2NHCH_2CH_2CH_2Si(OCH_3)_3$, abbreviated as AEAPTMS, 96%) was purchased from Alfa Aesar Co.

1.2.2 Synthesis of the SBA-15 Silica Substrate.

2-D hexagonal SBA-15 samples were synthesized following the method proposed by Choi et al.[23] Briefly, the steps for preparation of SBA-15 consist of dissolving 53.6 g of Pluronic P123 in 975 g of water and 29.75 g of HCl at room temperature overnight and then adding 86.7 g of TEOS into the resultant solution heated at 35 °C and further stirring it for 24 h. Following this, aging of the solution is conducted at 100 °C for 24 h. The resultant powder is filtered and dried for 24 h at 100 °C. The template is removed via calcination at 550 °C with a 1 °C/min heating rate. With this method, six batches of equivalent SBA- 15 (~22 g each) were produced and mixed, while identical structural properties for each batch have been confirmed by the characterization methods.

1.2.3 Preparation of the Functionalized Products.

The grafting technique was used to introduce the amine functionality, e.g., APTMS and AEAPTMS, into SBA-15. The amount of amine grafted in mesoporous material can generally be correlated to the amount of silanol groups present on the silica surface. Hence, SBA-15 was first rehydroxylated in order to break some of the Si-O-Si bridges and convert them into Si-OH. To achieve this, each batch of SBA-15 (~22 g) was stirred in 300 g of pure water at 85 °C for 7 h and then dried overnight at 100 °C in an oven. The ensuing grafting procedure consists of treating overnight under a vacuum a weighted quantity of SBA-15 in a multineck flask at 200 °C. This drying step is necessary to remove any physisorbed water or CO_2 that might have been adsorbed during the preparation or storage steps. Following this, a quantity of dry toluene (100 $cm^3/g_{support}$) is added to the dry silica powder placed into the multineck flask kept under argon. The temperature was raised up to 110 °C. A quantity

of APTMS or AEAPTES (1.0 $cm^3/g_{support}$) is then added, and the synthesis mixture is stirred for 24 h under reflux. After cooling, the modified materials are filtered and washed abundantly with toluene and hexane.

By means of this grafting technique, six batches (~6 g each) of APTMS grafted on SBA-15 and seven batches (~6 g each) of AEAPTMS grafted on SBA-15 were prepared and these will be referred to as APS (monoamine) and AEAPS (diamine), respectively.

1.2.4 Characterization Methods.

The nitrogen adsorption isotherms were measured at liquid nitrogen normal-boiling temperature (-196 °C) using a Micromeritics ASAP 2010 volumetric adsorption analyzer. Prior to measurements, the samples were outgassed under a vacuum for at least 5 h at 200 °C for the bare SBA-15 samples and 80 °C for the amine-grafted SBA- 15 samples. The Brunauer-Emmett-Teller (BET) equation was used to calculate specific surface area from adsorption data obtained at *P*/*P*0 between 0.05 and 0.2. Nonlocal density functional theory (NLDFT) methods with built-in software were used to calculate pore size distributions. In addition, the total pore volume was acquired from the amount of nitrogen adsorbed at P/P_0) 0.95, assuming that adsorption on the external surface was negligible compared to adsorption in pores. For all samples, the number of grafted amine moieties was determined from CHN elemental analysis performed on a Carlos Erba 1106 elemental analyzer. XRD patterns were recorded using a Siemens D5000 diffractometer equipped with Cu KR radiation (40 kV, 30 mA). XRD measurements were performed in the 0.8-3° range in 2-theta, under ambient conditions at 0.02° angular steps and 1.2 s per step dwell time.

1.2.5 Hydrolytic Stability of Grafted Amine on SBA-15.

The grafted amines on SBA-15 were subjected to eight immersion cycle tests in distilled water at 40 °C for 24 h. After each immersion cycle, samples were filtered and rinsed with 200 mL of toluene and hexane and then dried in a vacuum oven at 80 °C for 4 h. The grafted amine/water ratio (1.5 g/300 g) was held constant in all eight cycles. The recovered sample after each (#*x*) immersion cycle is abbreviated as C*x*-AEAPS or C*x*- APS (e.g., C4-AEAPS is the AEAPS sample recovered afterthe fourth immersion cycle). Moreover, the first four cycles of aforementioned procedure were repeated in a three-neck flask at 30 °C in which pH and electrical conductivity were monitored after introducing a weighted quantity of SBA-15 with grafted amine. It should be noted that the system was kept under an

argon atmosphere to avoid any changes in pH or conductivity and to prevent unwanted dissolution of adventitious CO_2.

1.2.6 Gas-Solid Adsorption.

Gas-solid adsorption studies were performed by using a Perkin-Elmer Diamond TG/DTA system. Both main and purge gases were maintained at 100 mL/min of UHP carbon dioxide and/or argon. A powdered sample of approximately 7 mg was loaded onto an alumina sample pan and exposed to argon flow from both main and purge flow. Afterward, the samples were heated up to 125 °C for 100 min to remove preadsorbed moisture and CO_2. Then, the sample was cooled down to 30 °C and left at this temperature for 45 min until sample mass stabilization was recovered. The mass recorded at this step was considered as the initial mass. In each of the following steps, the samples were exposed to CO_2 and/ or Ar flows at 30 °C for a period of 45 min (see Table 1). The mass of adsorbed CO_2 was calculated on the basis of the equilibrium mass measured at the end of each step. The effect of moisture on CO_2 adsorption was also determined using the same initial treatment procedure and subsequently exposing the sample to humidified gas. A relative humidity of 36% was obtained during these tests by passing the dry gas through a gas saturator that was held at a constant temperature. To decouple the adsorption of moisture from that of CO_2, samples were exposed to moist argon, after the initial activation, until water uptake had ceased. Then, the same steps for CO_2 and/or argon feeds were applied according to Table 1. It should be noted that this way of disentangling the mass contribution of adsorbed CO_2 from the total mass signal in moist conditions assumes no enhancement of water adsorption takes place due to amine- CO_2 chemistry nor water evaporation after moist flow has been disabled. This may be more an approximation than a definite statement, but we will nonetheless rely on it based on the online mass spectrometry monitoring of the signals stemming from the molecular ions H_2O^+ (m/z = 18) and CO_2^+ (m/z = 44).

Table 1. Argon and CO_2 Sweep Gases in TG/DTA

		step 1	step 2	step 3	step 4	step 5
main gas	CO_2 (mL/min)	50	75	100	100	100
	Ar (mL/min)	50	25	0	0	0
purge gas	CO_2 (mL/min)	0	0	0	50	100
	Ar (mL/min)	100	100	100	50	0
total flow	CO_2/Ar (mL/min)	200	200	200	200	200

1.2.7 Gas-Liquid Absorption and Gas-Liquid-Solid Adsorption/ Absorption.

Heterogeneous and homogeneous experiments were performed using the apparatus of gas-solid-liquid equilibrium (GSLE) illustrated in Figure 5. The setup was employed in our group previously for solubility measurements.[24,25] Considering the importance of monitoring pH, electrical conductivity, and temperature throughout the solubility experiments, the setup has been modified to host a conductivity meter, pH meter, and thermometer in a four-neck flask with specific connectors and adaptors that can withstand high vacuum during experiments. A thorough description of the apparatus and the method used are presented elsewhere[24] and briefly summarized in the Supporting Information section, focusing on the elements modified for the current study.

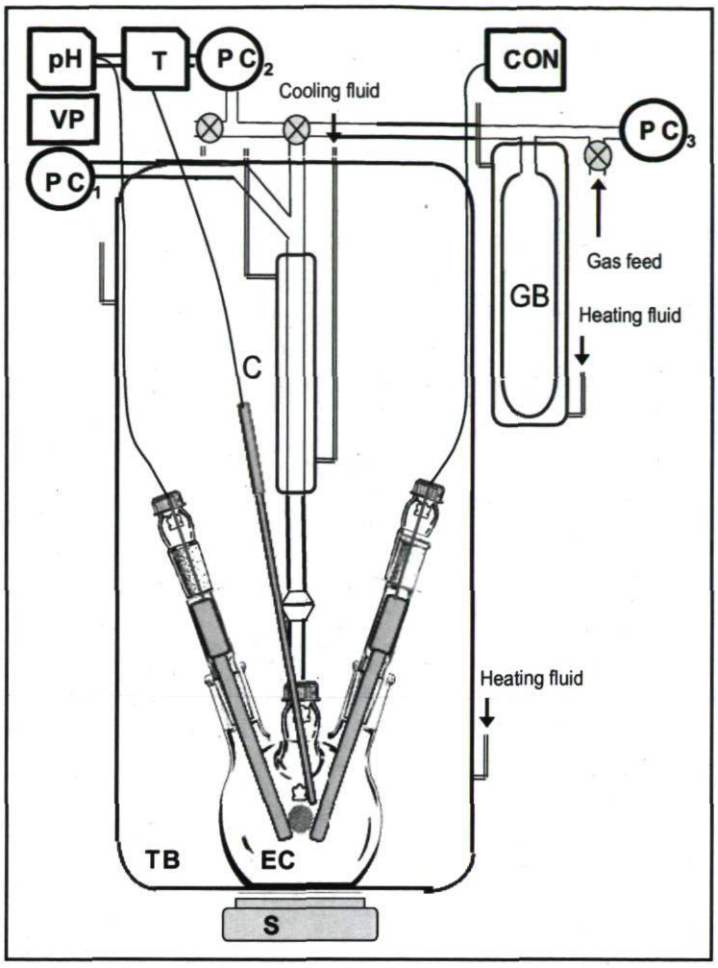

Figure 5. A schematic representation of the GSLE setup

1.3 Results and Discussions

1.3.1 Characterization of Materials.

N_2 sorption isotherms offresh (F-SBA-15), rehydroxylated substrates (SBA-15) and fresh powdered samples after amine grafting (F-APS and F-AEAPS) are illustrated in Figure 6. The characteristic type IV isotherm and H1-type hysteresis loop of SBA-15 remain unchanged after hydroxylation at 80 °C. Similarly for F-APS and F-AEAPS the materials show the same characteristic isotherm and hysteresis loop as the bare hydroxylated substrate. Surface characteristics along with CHN results of APS- and AEAPS-bearing sorbents are summarized in Table 2. The decrease in specific surface area, average pore diameter, and total pore volume of functionalized SBA-15 powder samples is reasonably attributed to the inclusion of the aminosilane groups grafted onto the pore walls of SBA-15.

Table 2. Characterization Data for Synthesized Materials[2]

	initial support properties			amount grafted	
	BET surface area (m^2/g)	pore diameter (nm)	pore volume (cm^3/g)	amine content (mmol(N)/g)	amine content (mmol(organic chain)/g)
F-SBA-15	760	8.2	0.98		
SBA-15	700	8.2	0.96		
APS 1	470	7.0	0.71	1.51	1.51
APS 2	520	7.0	0.79	1.56	1.56
APS 3	540	7.0	0.83	1.64	1.64
APS 4	510	7.0	0.78	1.58	1.58
APS 5	480	7.0	0.72	1.49	1.49
APS 6	520	7.0	0.78	1.51	1.51
APS (Mix)	510	7.0	0.77	1.60	1.60
AEAPS 1	490	6.8	0.79	2.84	1.42
AEAPS 2	530	7.0	0.86	2.55	1.28
AEAPS 3	390	7.0	0.63	2.87	1.44
AEAPS 4	350	7.0	0.57	2.75	1.38
AEAPS 5	420	7.0	0.68	2.84	1.42
AEAPS 6	430	7.0	0.70	2.63	1.32
AEAPS 7	400	7.0	0.65	3.10	1.55
AEAPS (Mix)	430	7.0	0.70	2.70	1.35

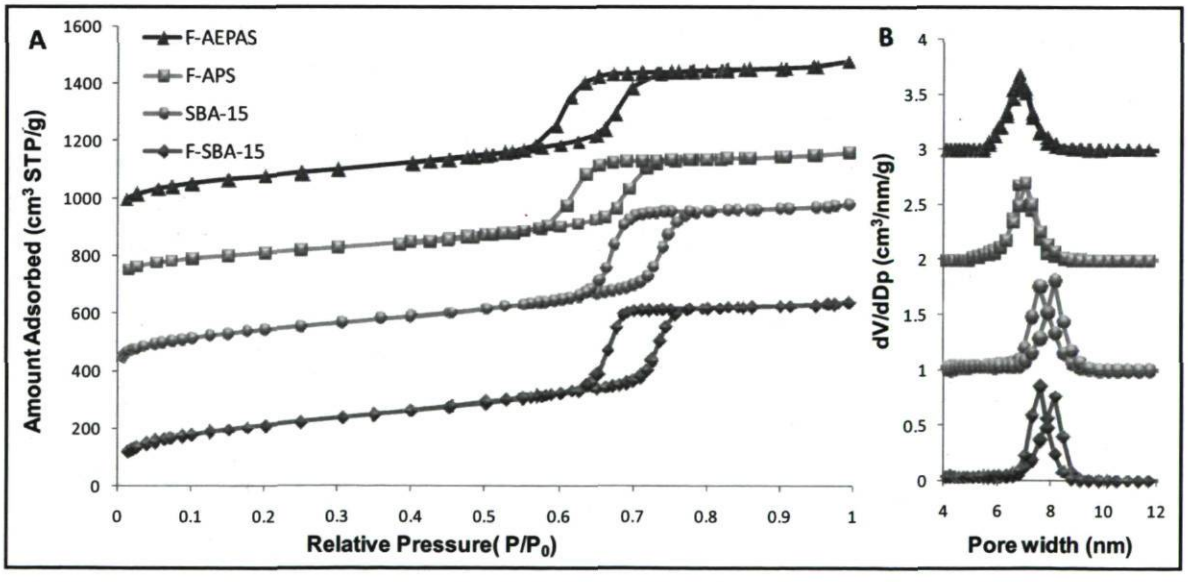

Figure 6. Nitrogen physisorption isotherms for F-SBA-15, SBA-15, F-AEAPS and F-APS measured at -196 °C. A: The isotherms for SBA-15, F-AEAPS and F-APS samples were offset vertically by 350, 700, and 950 cm^3 STP /g, respectively; B: The SBA-15, F-AEAPS and F-APS samples were offset vertically by 1, 2, and 3 cm^3 /nm /g, respectively.

[2] per unit mass of final product

1.3.2 Hydrothermal stability of grafted amine.

Hydrothermal Stability of Grafted Amines. F-APS and F-AEAPS were subjected to eight immersion cycles in water at 40 °C for 24 h to forge an objective measure of the strength of amine/SBA-15 association for which results are illustrated in Figure 7. It has been observed that maximum leaching occurred in the first two cycles, and then, the leaching slightly weakened during the third and fourth cycles. Thereafter, the nitrogen content of AEAPS remained more or less stable while leaching seemed to progress at a lower rate for APS. According to Asenath et al.,[26] possible anchoring modes of aminosilanes to the substrate to be envisioned are shown in Figure S1A of the Supporting Information. Two types of linkages are displayed: (i) strong covalent bonding between F-SBA-15 and the would be grafted, in principle leaching-proof, amine-bearing aminosilanols (Figure S1A-a,b, Supporting Information); (ii) weaker hydrogen-bonding-type interactions between the surface silanols and aminosilane silanols (Figure S1A-e, Supporting Information), the ethoxy (Figure S1A-f, Supporting Information), and the amine (Figure S1A-d, Supporting Information) moieties of the aminosilane molecules. Partial loss of grafted amines, especially in the earlier immersion cycles, may be attributed preferentially to those four latter weaker fixation events. However, another possibility causing leaching of grafted amines in aqueous media is through hydrolysis of the siloxane bonds between aminosilane and the silica substrate. The main process inducing degradation of amine is the breaking of the chemical bonds between the aminopropylsilane layer and the silica surface according to catalytic hydrolysis of siloxane bonds involving the amine function and a water molecule, which is shown schematically in Figure S1B of the Supporting Information.[27] As shown in Figure 7, the amine content for AEAPS drops from 1.35 to 0.82 mmol(organic chain)/g(final product) [or equivalently, 2.7 to 1.64 mmol (N)/g (final product)]. Afterward, degradation is virtually interrupted. Second, the rate of amine degradation decreased for APS after the fourth cycle but still continued until the eighth cycle. These observations are congruent with the fact that amine-catalyzed detachment can be minimized by controlling the length of the alkyl linker in aminosilanes.[26]

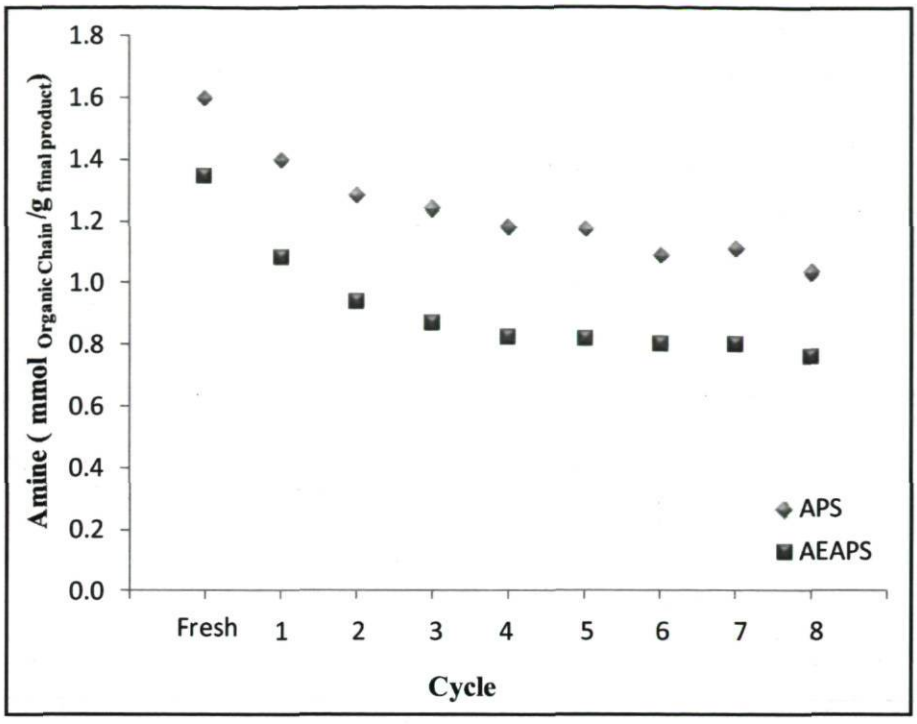

Figure 7. Hydrothermal stability test of APS and AEAPS in water

Another way of probing the hydrothermal stability of amine grafting on silica is to disperse the samples in distilled water and monitor the solution pH/electrical conductivity. Special care has been taken in order to avoid any contact with the atmosphere by imposing an argon headspace to prevent pH or electrical conductivity drifts by atmospheric carbon dioxide interferences. Qualitatively, one can assume that a stable material for which the basic molecules are retained immobilized inside the silica backbone would not show significant pH or electrical conductivity variations. Figures 8 and 9 represent the pH and electrical conductivity variations as a function of time for the first four immersion cycles of AEAPS in the aqueous phase. Insets in these figures highlight the short-term changes over 30 min time spans. Indeed, pH increased rapidly in the first five minutes before a plateau was reached, while electrical conductivity exhibited monotonic rises over the first 2-3 h before to resume on a slower-pace rising trend up to 24 h. Considerable variations in equilibrium electrical conductivity/pH values were observed in these four immersion cycles, showing major leaching occurred in the first cycle. The results are in agreement with the fact that the greatest decrease in amine content reported in Figure 7 coincides with the transition from fresh AEAPS and the first immersion cycle. In the third and fourth immersion cycles, the equilibrium electrical conductivity/pH values were very close to each other, although their deviations from electrical conductivity/pH values for pure water (conductivity = 2 μS/ cm at pH 7) can be attributed to the process of amine protonation in water. In fact, the aminosilane - NH_2 (or -NH-) groups should be fully protonated at pH < 9.[28]

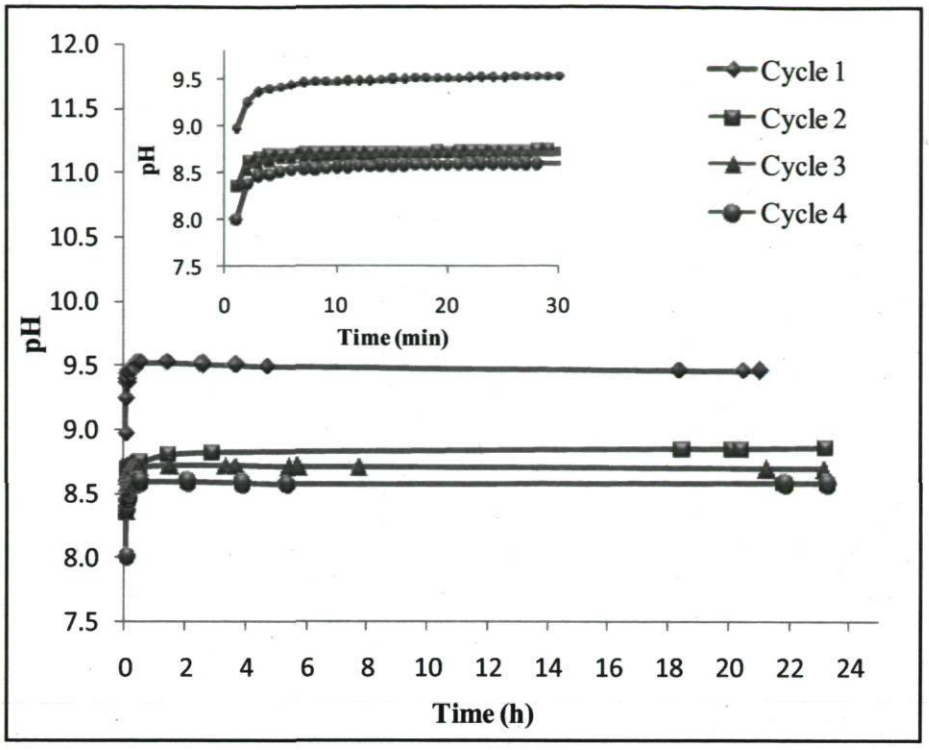

Figure 8. pH vs time profile measured at first four immersion cycles

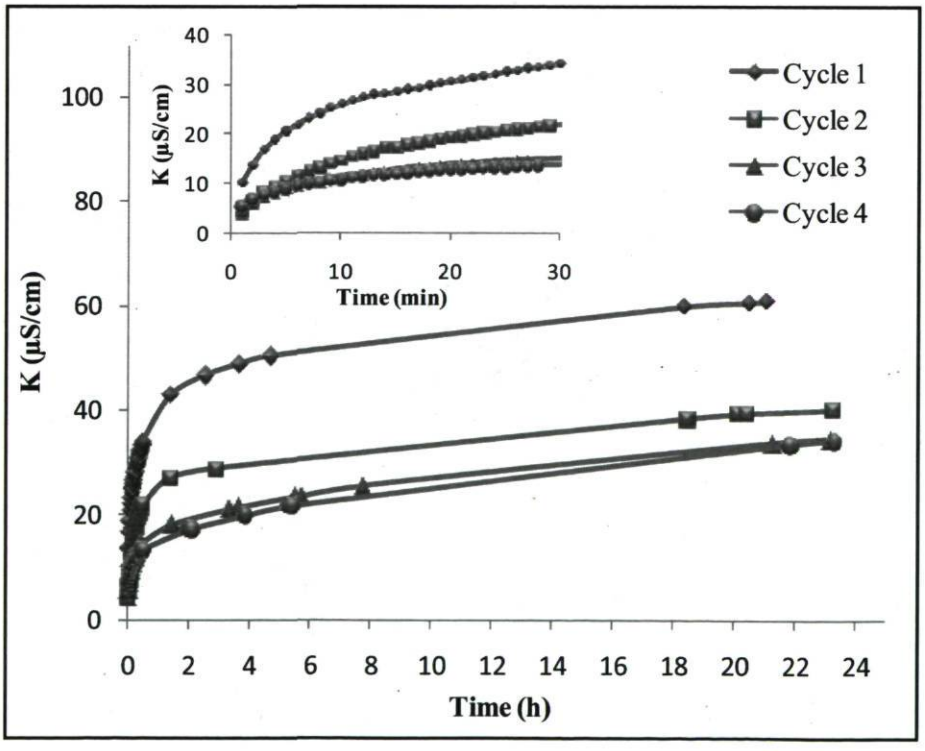

Figure 9. Conductivity vs time profile measured at first four immersion cycles

To gain further insights into the hydrothermal stability of the mesoporous structures after several immersion cycles, XRD and nitrogen adsorption-desorption isotherms were performed. The XRD patterns of SBA-15, F-APS, C4-APS, C8-APS, F-AEAPS, C4-AEAPS, and C8-AEAPS showed well-resolved peaks that can be indexed as the diffraction planes (100), (110), and (200) due to the hexagonal array of SBA-15 mesopores (not shown), indicating that well-ordered mesostructures have been retained after functionalization and these mesoporous structures are preserved after several prolonged immersions in water. Figure 10 displays the nitrogen sorption isotherms of C4-APS, C8-APS, C4-AEAPS, and C8-AEAPS. Apart from C8-AEAPS, the samples exhibit isotherms with a well-developed step in the relative pressure (P/P_0) range 0.65-0.80 characteristic of capillary condensation in large uniform mesopores. The isotherm trends suggest that the samples possess mesostructural ordering with fairly narrow pore size distributions, as observed in the fresh material. In the case of C8-AEAPS samples, increasing the number of immersion cycles broadened the pore size distribution without destroying the framework mesoporosity (Figure 10). The increase in the pore size and volume of C4- APS and C4-AEAPS, as tabulated in Table 3, might be due to the leaching process or, as suggested by Mokaya et al.,[29] probably a result of pore wall thinning through partial pore wall dissolution. According to Figure 7, maximum amine leaching occurred in the first two cycles; thus, the increase in pore size and volume of C8-APS and C8-AEAPS may be merely attributed to pore wall dissolution.

Table 3. Characterization Data for the Materials Used In Hydrothermal Stability Test

	initial support properties		
	BET surface area (m^2/g)	pore diameter (nm)	pore volume (cm^3/g)
C4-APS	430	8.3	0.91
C8-APS	490	8.5	1.07
C4-AEAPS	450	7.9	0.80
C8-AEAPS	460	8.8	1.13

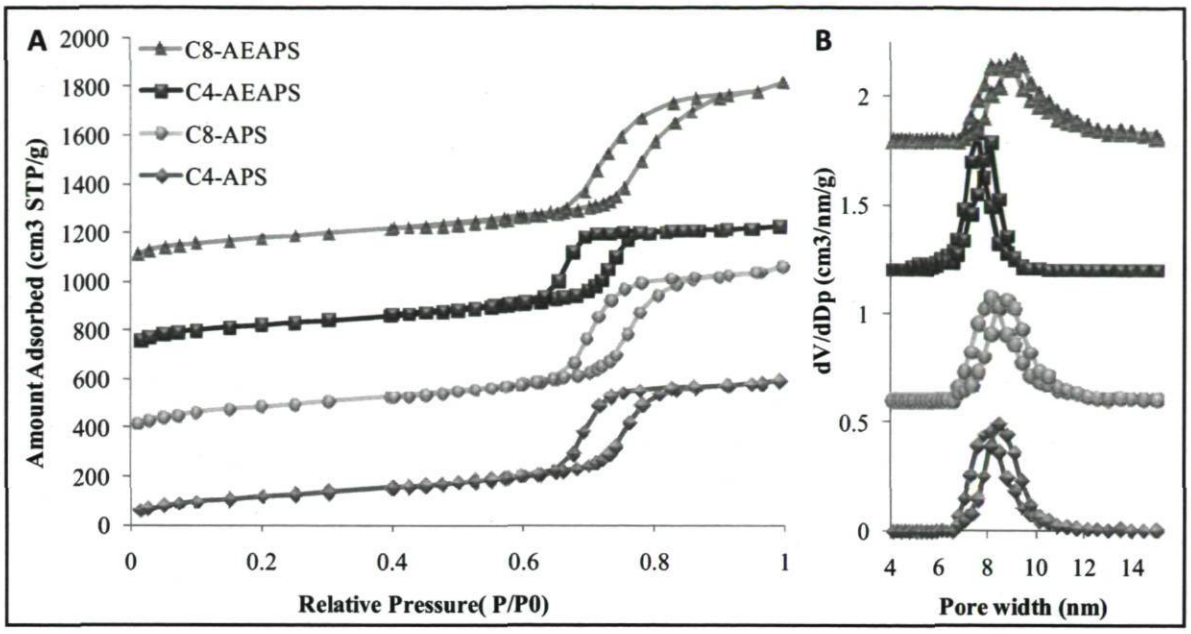

Figure 10. Nitrogen physisorption isotherms for materials used in hydrothermal stability test. A: The isotherms for C8-APS, C4-AEAPS and C8-AEAPS samples were offset vertically by 350, 700, and 1050 cm^3 STP /g, respectively; B: The C8-APS, C4-AEAPS and C8-AEAPS samples were offset vertically by 0.6, 1.2, and 1.8 cm^3 /nm /g, respectively.

1.3.3 Gas-Liquid Absorption & Gas-Liquid-Solid Adsorption/ Absorption.

The proper operation of the apparatus (GSLE) and the accuracy of the measuring method were verified by studying the solubility of carbon dioxide in pure water at different temperatures between 20 and 30 °C. Data expressed in terms of Henry's law constants are presented in Table 4, in comparison with the literature data for the solubility of CO_2 in water. Very good agreement with an average deviation of about 1% was found that allows us to consider both the apparatus and resulting data reliable.

A series of CO_2 solubility experiments was conducted at 30°C for CO_2 partial pressures ranging from 15 to 105 kPa according to the following steps:

1- Measuring the CO_2 capture capacity of SBA-15-grafted amines for two slurry concentrations of 2 and 5 g of fresh APS (F-APS) and AEAPS (F-AEAPS) in 230 g of double-distilled water (referred to as the *heterogeneous route* or Ht).

2- Measuring the CO_2 absorption capacity of aqueous amines with equivalent amine concentrations considered in the heterogeneous route (namely, the *homogeneous route* or Hm).

In order to compare the results, the (homogeneous) aqueous amines tested in our experiments (AP and AEAP) were chosen to have almost identical molecular structures as the grafted amines (Figure S2, Supporting Information).

3- Measuring CO_2 absorption capacity of double-distilled water (230 g), i.e., pure physical absorption.

The physical solubility of CO_2 in pure water was considered as a base for comparison to specify the effect of the presence of amines in heterogeneous and in homogeneous routes.

4- Measuring CO_2 capture capacity of two slurry concentrations of unfunctionalized (i.e., bare) SBA-15 in 230 g of double distilled water.

The hydroxyl groups (Si-OH) on the SBA-15 surface have the potential to adsorb CO_2. Though the amine grafting reactions would have depleted a great deal of the available Si-OH, the residual noncoupled hydroxyl groups might still have an effect on CO_2 adsorption capacity. Hence, to decouple the effect of hydroxyl groups from the amine groups in the total adsorbed CO_2, a set of experiments was conducted using a slurry of bare SBA-15. The concentrations of these slurries were determined by multiplying the weight ratios of SBA-15/F-APS or SBA- 15/F-AEAPS by the concentrations considered in the heterogeneous conditions (i.e., 2 and 5 g of grafted amine in 230 g of water). TGA-MS measurements allowed for a quantitative determination of the weight ratios by heating the samples under an oxygen stream in two consecutive steps. In the first step, the samples were heated up to 150 °C for 4 h to remove preadsorbed moisture during storage, and thereafter, the temperature was increased up to 800 °C, where it was maintained for 8 h in order to ensure full combustive removal of the sorbent organics content. The results revealed that the weight ratios of SBA-15/ F-APS and SBA-15/F-AEAPS were, respectively, 0.80 and 0.85. The same quantity of bare SBA-15 was used in comparison with the tests with grafted-amine SBA-15. Although this choice does not rigorously reflect equal amounts of hydroxyl groups for the two situations, the solubility tests with bare SBA-15 thus performed were used to approximate the physical adsorption contribution out of the total adsorbed CO_2 in the slurry consisting of the grafted-amine materials.

Table 4. Henry's law constant for CO_2 in water and comparison with literature values

T (°C)	H (Pa m^3/mol)	deviation (%)	reference
20	2631.6	0.87	32
	2647.0	1.44	33
	2589.9	0.73	34
	2638.2	1.12	35
	2608.8		this study
25	2967.4	0.23	32
	2993.0	1.09	35
	2984.0	0.79	34
	2960.4		this study
30	3314.0	0.40	33
	3382.0	2.40	36
	3394.4	2.76	34
	3300.7		this study

The total adsorbed CO_2 was expressed as pseudomolality in moles of CO_2 per unit mass of water, merging altogether the chemisorbed/physisorbed contributions on the sorbent surface and the portion absorbed within the slurry liquid in the heterogeneous route and the chemically/physically absorbed contributions of amine solution in the homogeneous route. It was plotted as a function of the equilibrium CO_2 partial pressure for the four aforementioned sets of experiments in Figures 11 and 12 for the mono- and diamine cases, respectively. It can be concluded that, for equal amine concentrations, liquid amines are more active than the ones grafted on mesoporous material. Indeed, 8 (or 3.2) mmol N/230 g from AP (Hm) yields a larger CO_2 equilibrium pseudomolality than an equal number of N moles stemming from heterogeneous APS (Ht), as shown in Figure 11. Similar qualitative trends hold true for the AEAP versus AEAPS comparisons (see Figure 12). Moreover, some slight differences in total adsorbed CO_2 were measured in pure water and in the slurry in the case of unmodified SBA-15 over a similar CO_2 partial pressure range at equilibrium. These small increments have been attributed to physisorbed CO_2 on SBA-15. In addition, almost identical amounts of adsorbed CO_2 were observed for two different SBA- 15 concentrations, providing postfacto evidence of the low ability of SBA-15 free hydroxyl groups to fixate meaningful amounts of CO_2 when bare SBA-15 is slurried in water. The contribution of physisorption of CO_2 on unfunctionalized SBA- 15 is thus considered nonsignificant.

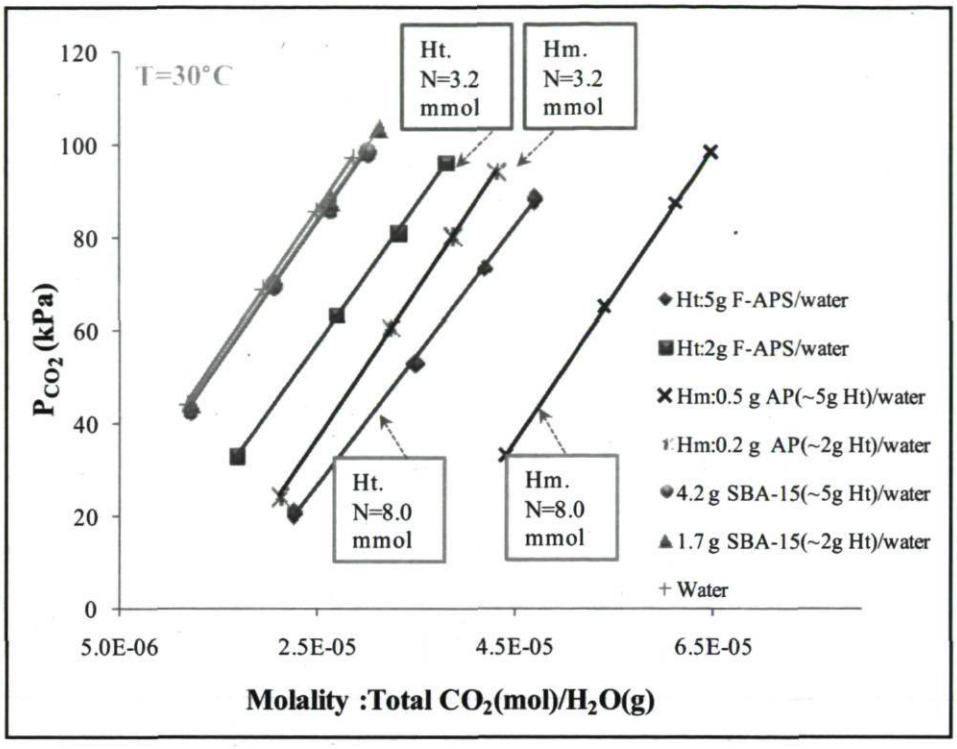

Figure 11. Total captured CO_2 in solution/slurry of F-APS, AP and SBA-15 in 230 g of water versus CO_2 partial pressure.

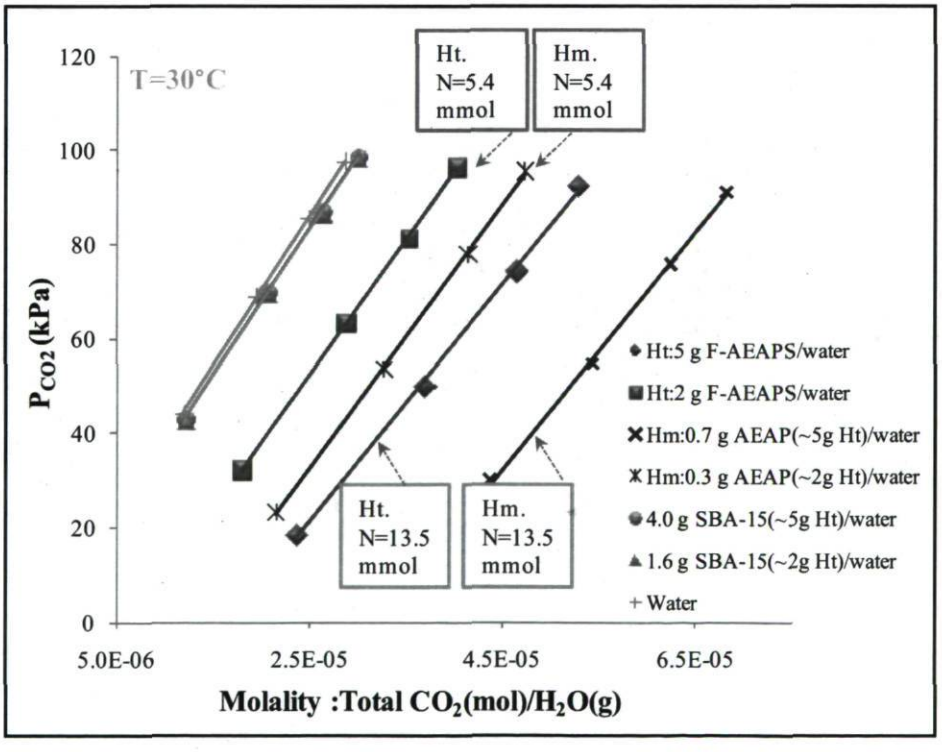

Figure 12. Total captured CO_2 in solution/slurry of F-AEAPS, AEAP and SBA-15 in 230 g of water versus CO_2 partial pressure.

Figure 13 displays the initial (before adding CO_2, shown as values lying on the *x*-axis) and the equilibrium pH/electrical conductivity versus CO_2 equilibrium partial pressure corresponding to the experiments discussed in Figures 11 and 12. It is interesting to note that, in both heterogeneous and homogeneous cases, the equilibrium pH values for both mono- and diamine are reported to revolve around 6 to 7 regardless of the level of the CO_2 equilibrium pressure and despite the quite different starting pH values (Figure 13A,C). In the case of electrical conductivity, mono- and diamine exhibited different behaviors (Figure 13B,D). For monoamine solution (Hm)/slurry (Ht), the electrical conductivity increased sharply with increasing CO_2 equilibrium pressure before a conductivity plateau was reached that was insensitive to higher equilibrium CO_2 pressures. On the contrary, diamine solution (Hm)/slurry(Ht) exhibited a progressive increase in electrical conductivity as a function of rising CO_2 equilibrium partial pressures. However, at high CO_2 partial pressure, the values observed in both mono- and diamine seemed practically the same.

As described above in the hydrothermal stability section, immersion in water of fresh-grafted amine sorbents drove a number of amine species into solution due to amine leach-off especially over the first soaking stages. As a result, in order to objectify the *genuine* contribution by the grafted amines out of the total amount of CO_2 captured in the heterogeneous experiments, the contribution of the leached amines (homogeneous pathway) in conjunction with the pH prevailing in the slurry should be recognized. Hence, a superposition principle was assumed to simplify the determination of each partial contribution. In each heterogeneous experiment, a leached amine was assumed to react according to similar paths as aqueous amines. To determine the quantity of leached amine, the nitrogen content of the grafted amines was measured by elemental analysis before and after each heterogeneous experiment. Therefore, a series of new experiments was conducted with leached amine concentrations in 230 g of water using AP and AEAP, in order to simulate the effect of leached amine in capturing CO_2. The difference obtained from total captured CO_2 in these homogeneous experiments and from pure water, over the whole range of CO_2 partial pressures tested in this study, would represent an estimate of the contribution of the leached amine to the total captured CO_2 in the heterogeneous experiments. Similarly, the effect of unmatched surface hydroxyl groups in adsorbing CO_2 was calculated from the difference of total captured CO_2 obtained in the corresponding experiment using bare SBA-15 in water and pure water over the whole range of CO_2 partial pressures. Since the solubility contributions from SBA-15, leached amine, and water can be known; the part left in the solubility for the heterogeneous experiments would be the contribution to solubility of CO_2 due to the grafted amines only.

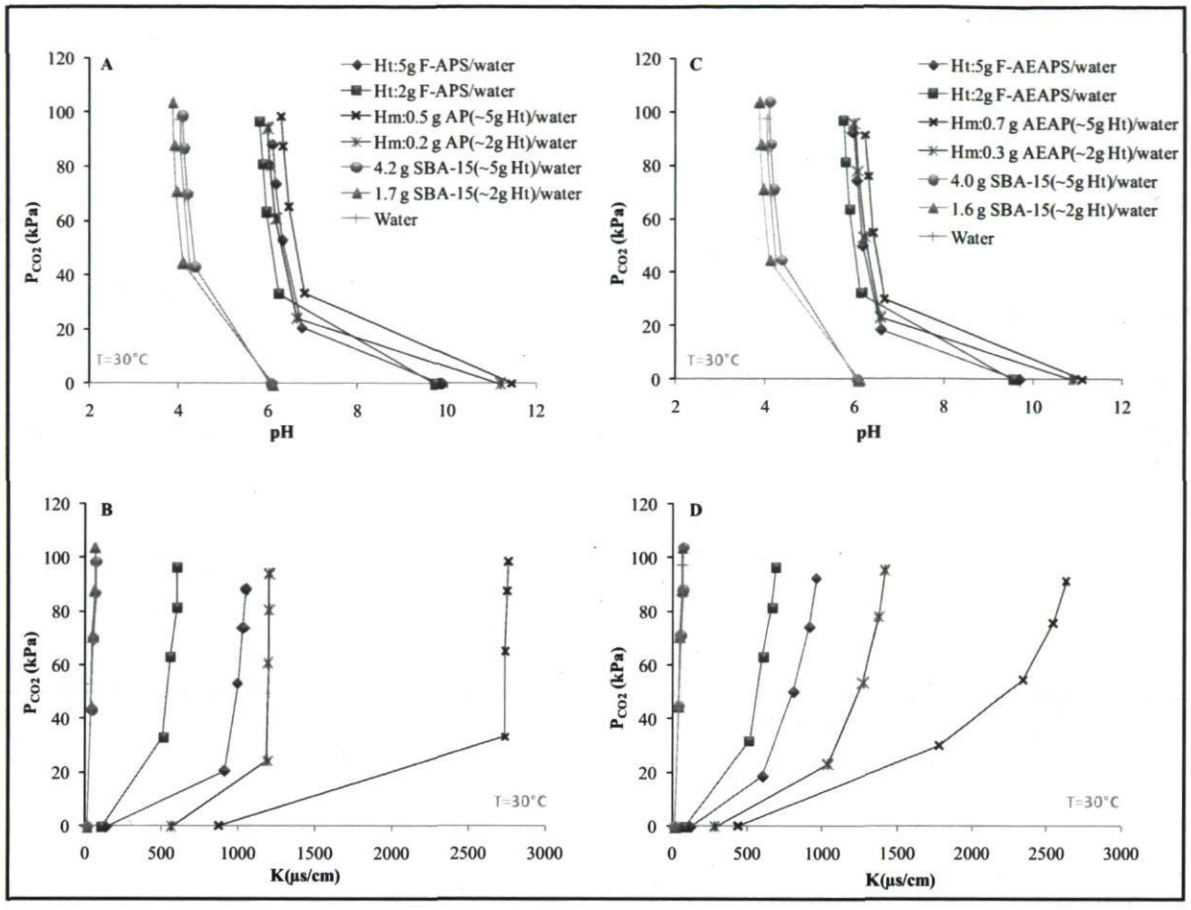

Figure 13. Equilibrium pH and conductivity in solution/slurry of (A, B): F-APS, AP and SBA-15; (C, D): F-AEAPS, AEAP and SBA-15 in 230 g of water versus CO_2 partial pressure.

In Figures 14 and 15, the contributions emanating from every part are illustrated for one amine concentration, i.e., 5 g of grafted amine in 230 g of water, using the F-APS and F-AEAPS in water, respectively. Due to the low amine concentration in play, pure water had the highest contribution, while the sorbent hydroxyl groups showed the lowest contribution in the total captured CO_2. In these two figures, SBA-15, H_{GA}, H_{LA}, water, and H_{total} stand for the sorbent hydroxyl groups, the grafted amines, the leached off amines, pure water (i.e., pure physical absorption), and the total solubility effects, respectively.

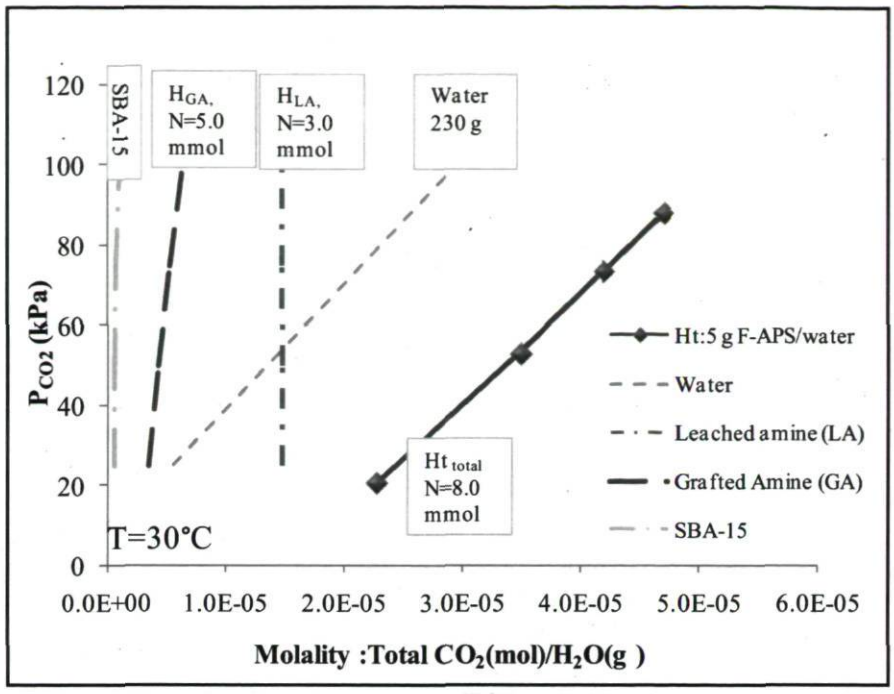

Figure 14. Contribution of water, SBA-15, leached amine and grafted amine in total captured CO_2 of F-APS in water.

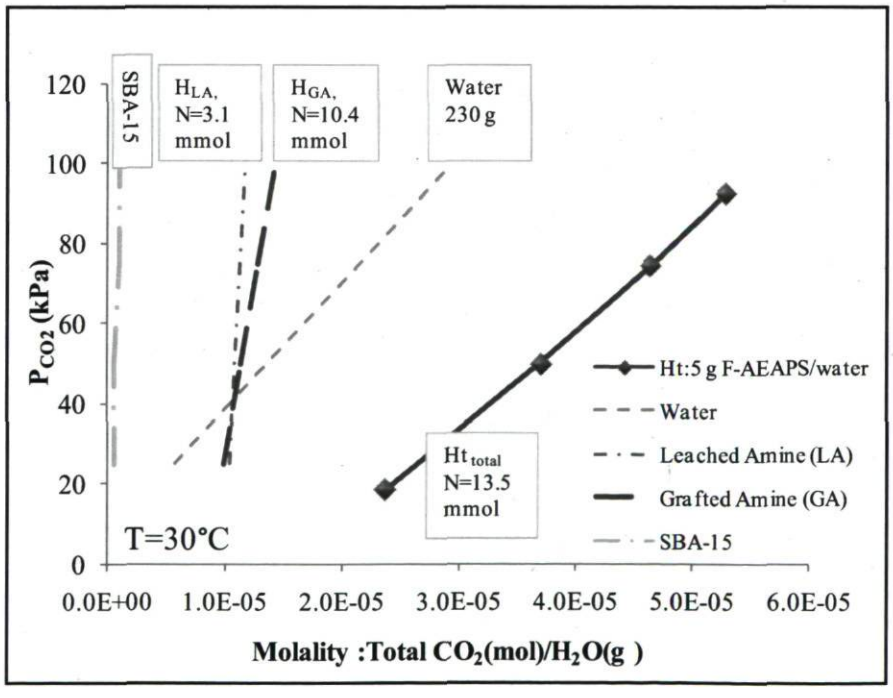

Figure 15. Contribution of water, SBA-15, leached amine and grafted amine in total captured CO_2 of F-AEAPS in water.

According to Figure 7, one can assume that negligible amounts of amine leach from AEAPS after the fourth immersion cycle in water. Hence, in order to reduce the effect of water and eliminate the presence of leached amine, a set of experiments was conducted at 30 °C over CO_2 partial pressures ranging from 15 to 105 kPa according to the following steps:

1- Measuring CO_2 capture capacity of grafted amines in three slurry concentrations of 2, 5 and 7 g of C4-AEAPS (4 cycle washed F-AEAPS) in 40 g of double-distilled water.

2- Measuring CO_2 absorption capacity of liquid amines with equivalent amine concentrations considered in step 1.

3- Measuring CO_2 absorption capacity of double-distilled water (40 g), i.e., pure physical absorption.

4- Measuring CO_2 capture capacity of three slurry concentrations of unmodified SBA-15 in 40 g of double-distilled water.

The SBA-15 concentrations were calculated on the basis of a weight ratio of SBA-15/C4-AEAPS equal to 0.92. The results are illustrated in terms of total captured CO_2 as a function of CO_2 partial pressure in Figure 16. Comparing the amount of CO_2 captured by diamine in heterogeneous and homogeneous conditions with almost identical amine structure and similar concentration, it is reasonable to assume that the lower adsorption capacity in the heterogeneous conditions might be due to the lower amine accessibility as caused by competitive pore volume filling with water. To produce quantitative effects in the heterogeneous route commensurate with the homogeneous route, more grafted amines would be required and thus correspondingly larger amounts of sorbents.

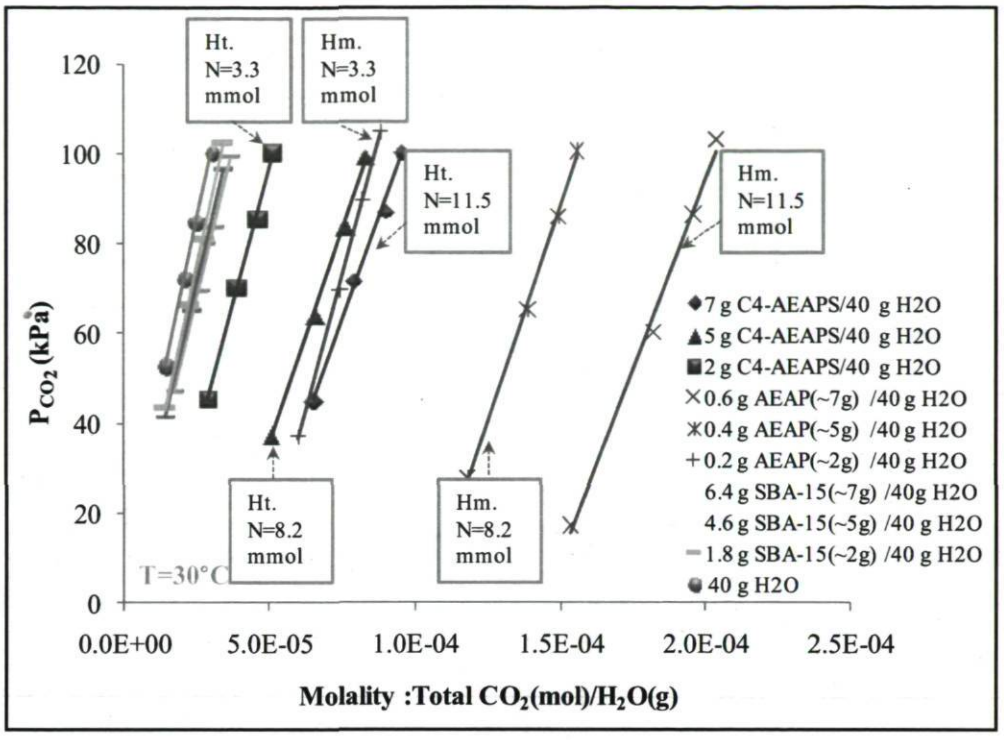

Figure 16. Total captured CO_2 by C4- AEAPS, AEAP and SBA-15 in 40 g of water in different CO_2 partial pressure.

1.3.4 Gas-Solid Adsorption

The effect of CO_2 partial pressure on the adsorption capacity of SBA-15, F-AEAPS, and C4-AEAPS was studied by TG-MS under both humid and dry conditions. The results shown in Figure 17 indicate that, by decreasing the sample nitrogen content from F-AEAPS (2.7 mmol N/g(final product)) to C4-AEAPS (1.64 mmol N/g(final product)) and unmodified SBA-15, the adsorption capacities diminished, accordingly. It is also observed that, for each sample, the difference between values measured in the presence of dry and humid CO_2 increased considerably by depleting the nitrogen content of the sorbent. Physical adsorption of CO_2 could play an important role in the total adsorption capacities of the samples in contact with dry CO_2. Conversely, on the basis of diffusional considerations and van der Waals molecular diameters, water uptake under humid conditions would plausibly proceed faster than the uptake of CO_2, attributing the majority of adsorbed CO_2 to chemical rather than to physical adsorption. That would explain why SBA-15 showed the lowest adsorption capacities in the presence of water vapor, though the same material in contact with dry CO_2 exhibits better results over the CO_2 partial pressure range under study. Chemical interactions of CO_2 with amines in C4-AEAPS narrow the gap between the amount adsorbed in the presence of dry and humid

CO_2 and as the amine content increased further (F-AEAPS). Not only did the gap disappear, but also the adsorption capacity in the presence of water vapor surpassed the results obtained under dry conditions. In fact, this could be expressed as chemical adsorption enhancement in the presence of water vapor compared to dry CO_2.

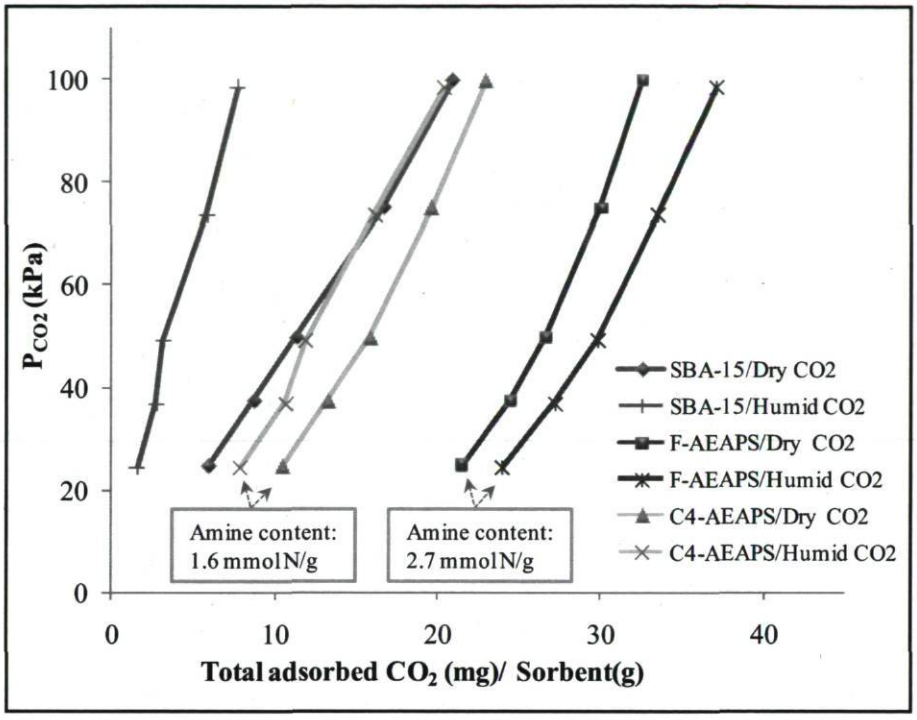

Figure 17. Total adsorbed CO_2 by F- AEAPS, C4- AEAPS and SBA-15 in contact with humid and dry CO_2.

1.3.5 Adsorption Efficiency of Grafted and Non-Grafted Amine

On the basis of the results obtained in previous sections, a comparison was done between CO_2 captured by grafted and nongrafted amine (C4-AEAPS, AEAP) in heterogeneous, homogeneous,and gas-solid adsorption conditions. Under comparable conditions in heterogeneous and homogeneous experiments, the contribution of pure water was subtracted from the total captured CO_2. It is worth mentioning here that C4-AEAPS in contact with water did not leach significantly its amine content. The results are presented in Figure 18, which indicates that the grafted amine adsorption efficiency, defined as the number of captured carbon dioxide molecules per nitrogen atom of amine, is not considerably influenced in the presence of liquid water as compared to the dry or humid conditions of gas-liquid adsorption. On the other hand, since the accessibility of amine groups is restricted by grafting them on SBA-15, their adsorption efficiency was significantly decreased compared to equivalent liquid amines. The influence of CO_2 partial pressure in the adsorption capacity of C4-

AEAPS under heterogeneous conditions was found to be much less than gas-solid adsorption. For example, at CO_2 partial pressures of 25 kPa, adsorption capacities of 300, 178, and 236 $\mu mol/g_{sorbent}$ and, at 100 kPa, 413, 464, and 522 $\mu mol/g_{sorbent}$ were, respectively, reported for C4-AEAPS in the presence of liquid water, moisture, and dry CO_2.

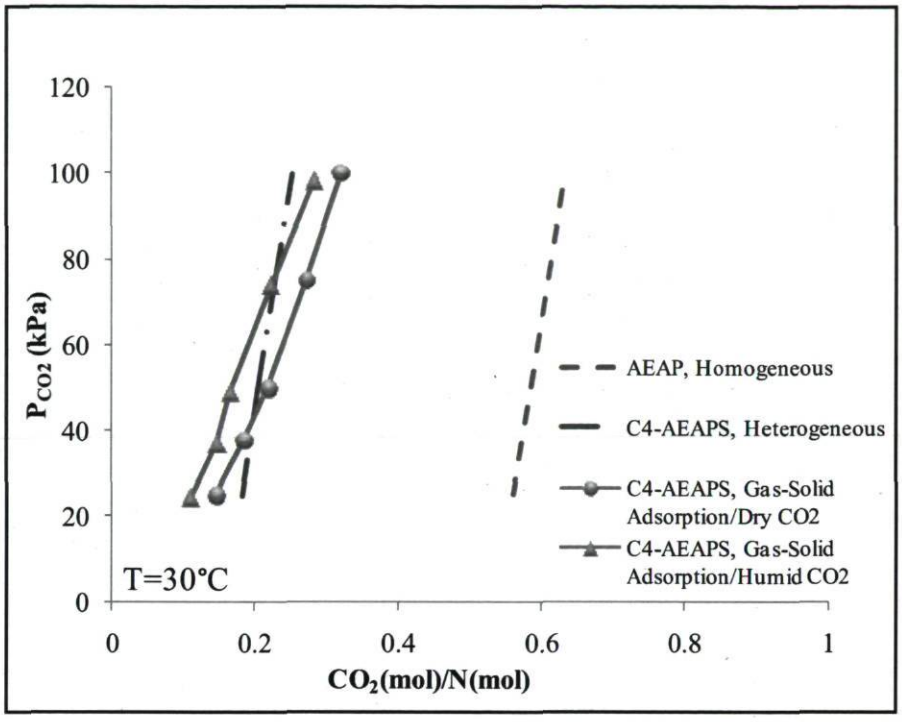

Figure 18. Adsorption efficiency of grafted and non-grafted amine in heterogeneous, homogeneous and gas-solid adsorption conditions.

1.4 Conclusions

Hydrothermal stability of APS and AEAPS was examined by subjecting the samples to eight immersion test cycles in water at 40 °C. The results revealed that maximum leaching occurred in the first two immersion cycles, while the nitrogen content of AEAPS remains more or less stable after the fourth immersion cycle, although a little instability was observed in almost all APS tests. Nitrogen sorption isotherms of C4-APS, C8-APS, C4-AEAPS, and C8-AEAPS confirmed that the mesoporous structures of APS and AEAPS were retained during prolonged contact with liquid-state water. Moreover, in equal amine concentrations, the CO_2 capture efficiencies of (identicalstructure) amines were compared in homogeneous, heterogeneous, and gas-solid adsorption over humid and dry conditions. The results revealed that aqueous amines are more active than the ones grafted on mesoporous materials. In addition, at low CO_2 partial pressure, the adsorption efficiency of C4-AEAPS

in the presence of liquid water surpassed the results obtained in the presence of humid and dry CO_2 of gas-solid adsorption, while by increasing the CO_2 partial pressure the effect of physical adsorption in mesoporous structure which is most dominant under dry conditions outperformed it over the result obtained in the presence of moisture and liquid water. Under heterogeneous conditions, the adsorption capacity of the C4- AEAPS (1.6 mmol N/g) varied within 300-413 μmol/g depending on the CO_2 partial pressure. Since the adsorption capacity of more than 1000 μmol/g is required for the reduction of CO_2 emission at large scale in an economic manner,[30] further increase in capacity is still necessary. Considering the low amine content of C4-AEAPS due to ~40% leaching in contact with water, it is conceivable that modifying the amine groups with the purpose of controlling the leaching process and increasing the amine content31 could bring the CO_2 sorption capacity up to the level for an appeal for industrial applications. It is also worth mentioning that, according to this research, grafted amine adsorption efficiency is not considerably influenced by the presence of liquid water compared to dry conditions in gas-solid adsorption, which represents a major advantage over adsorbents that even need stringent moisture control in their gas stream. Hence, it is conceivable that applying grafted amines inside the scrubber with slight water circulation could remedy the problems of using aqueous amine in conventional gas-liquid scrubbers.

Acknowledgment

Financial support from FL Canada Research Chair "*Green processes for cleaner and sustainable energy*" and F.K. Canada Research Chair "*Functional nanostructured materials*" and the Discovery Grants to F.L., F.K., and M.C.I. from the Natural Sciences and Engineering Research Council (NSERC) is gratefully acknowledged.

Nomenclature and Acronyms

AEAP: 2-Propylaminoethylamine

AEAPTES: N-(2-Aminoethyl)-3-(aminopropyl) triethoxysilane

AEAPTMS: N-(2-Aminoethyl)-3-(aminopropyl) trimethoxysilane

AP: 1-Aminopropane

APTES: 3-(Aminopropyl)triethoxysilane

APTMS: 3-(Aminopropyl)trimethoxysilane

C: Condenser

CON: Conductivity meter

CX-AEAPS: AEAPS sample recovered after Xth immersion cycle in water

CX-APS: APS sample recovered after Xth immersion cycle in water

F-AEAPS: Fresh AEAPS

F-APS: Fresh APS

F-SBA-15: Fresh SBA-15

EC: Equilibrium Cell

GB: Gas Burette

GSLE: Gas-Solid-Liquid Equilibrium apparatus

$n_{G,fin}$: Number of moles of gas left in the equilibrium cell headspace

$n_{G,in}$: Number of moles of gas added to the equilibrium cell

$n_{G,ab}$: Number of moles of gas ab/adsorbed in the solution/slurry

n_G: Number of moles in gas burette

PC: Pressure Capture

pH: pH meter

P_G: Pressure of gas burette

P_{tot}: Total pressure of the equilibrium cell headspace

P_{VS}: Vapor pressure of gas-free solution/slurry

S: Magnetic Stirrer

T: Thermometer

TA: (3-trimethoxysilylpropyl)diethylenetriamine

TA1:3-[2-(2-aminoethylamino) ethylamino]propyltrimethoxysilane

TB: Thermostated Bath

T_G: Temperature of gas burette

V_{EC}: Cell volume

$V_{G, EC}$: Volume of the equilibrium cell headspace

V_{GB}: Volume of gas burette

VP: Vacuum Pump

1.5 Supporting Information

Gas-liquid absorption & gas-liquid-solid adsorption/absorption.

The equilibrium cell consisting of a 250 mL four-neck flask ensured, by means of good agitation, an appropriate gas-liquid-solid or gas-liquid contacting. Conductivity and pH meter were designed to enter completely into the four neck flask each with the aid of 20 cm connector. Each probe, inside the flask, was connected to its transmitter via a cable that passes through a vacuum tight adapter. A vacuum tight seal was equipped with the compression cap and Viton O-ring to allow adjustable immersion of the probes. The equilibrium cell was connected to the condenser by means of a grease-free ball joint fitted with corrosion resistant silicone O-rings. The condenser was optimized in order to practically avoid solvent loss during the degassing procedure. As the accuracy of the solubility measurements depends on accurate measurements of the total pressure inside the equilibrium cell, the gas pressure in the equilibrium cell was measured by means of a temperature-controlled MKS Baratron type 628B absolute pressure transducer (precision 0.25% full scale, measurement resolution 0.001% full scale). The Baratron transducer avoids vapor condensation during measurements and allows very accurate determinations of the total pressure. Both undissolved gas and solvent vapor pressures in the flask headspace were determined. The equilibrium cell together with the condenser and the connecting lines up to the Baratron transducer were kept at a constant temperature using a thermostated bath controlled within ±0.01K.

Electrical conductivity meter (Eutech, alpha CON 500, precision ±1% of full scale reading in respective range) was used with an electrode (Cole-Parmer, K=1.0, 100 Ohm Pt RTD ATC) which was calibrated using commercial calibration solutions. pH meter (Eutech, alpha pH 500, precision ± 0.01 pH) was also connected to a pH electrode (Sensorex Corp, epoxy body combination) that was calibrated using commercial standard buffers at *pH* 4, 7 and 10. Consequently, the experimental uncertainty in the measured solubility data was estimated to be about ±1%.

The experiment started by preparing the amine solution (respectively, grafted amine slurry) by weighing a quantity of amine (respectively, grafted amine) and double distilled water using a Mettler Toledo AB204 balance with a precision of ±0.0001 g.

A known mass of solution (respectively, grafted amine slurry) was introduced into the equilibrium cell and then slowly degassed by stirring under vacuum until the base pressure of the vacuum pump was reached. A high contact surface condenser where an ethylene glycol–water mixture at −6 ◦C circulated was used to avoid the solvent loss during the degassing procedure. After completion of degassing, the

equilibrium cell was sealed and temperature was assigned a set point T at which the solubility was to be measured. The vapor pressure P_{VS} of the gas-free solution (respectively, grafted amine slurry) was measured after the system had equilibrated. The carbon dioxide was added into a thermostated gas burette of volume V_{GB} maintained at temperature T_G, and the pressure P_{G1} was read. The number of moles n_{G1} of gas in the burette was computed as:

$$n_{G1} = \frac{P_{G1} V_{GB}}{R T_G} \tag{1}$$

After introducing a certain amount of gas into the equilibrium cell, a new pressure P_{G2} in the burette was read and the number of moles of gas remaining in the gas burette was calculated:

$$n_{G2} = \frac{P_{G2} V_{GB}}{R T_G} \tag{2}$$

The difference n_{G1}-n_{G2} (= $n_{G,in}$) represents the number of moles of gas added to the equilibrium cell where the solution (respectively, grafted amine slurry) was vigorously stirred until reaching equilibrium, as characterized by a constant pressure readout corresponding to the total (gas + solvent vapor) pressure. The gas partial pressure was determined after subtracting the solution (respectively, grafted amine slurry) vapor pressure P_{VS} from the total pressure P_{tot}. This allowed retrieving the number of moles $n_{G,fin}$ of gas left in the equilibrium cell headspace from Eq.(3) whereas the number of moles of gas ab/adsorbed in the solution (respectively, grafted amine slurry) at equilibrium $n_{G,abs}$ was determined according to Eq.(4):

$$n_{G,fin} = (P_{tot} - P_{VS}) \frac{V_{G,EC}}{RT} \tag{3}$$

$$n_{abs} = n_{G,in} - n_{G,fin} \tag{4}$$

The headspace volume of the equilibrium cell $V_{G,EC}$ is given by the difference between the cell geometrical volume V_{EC} and that occupied by the solution (respectively, grafted amine slurry).

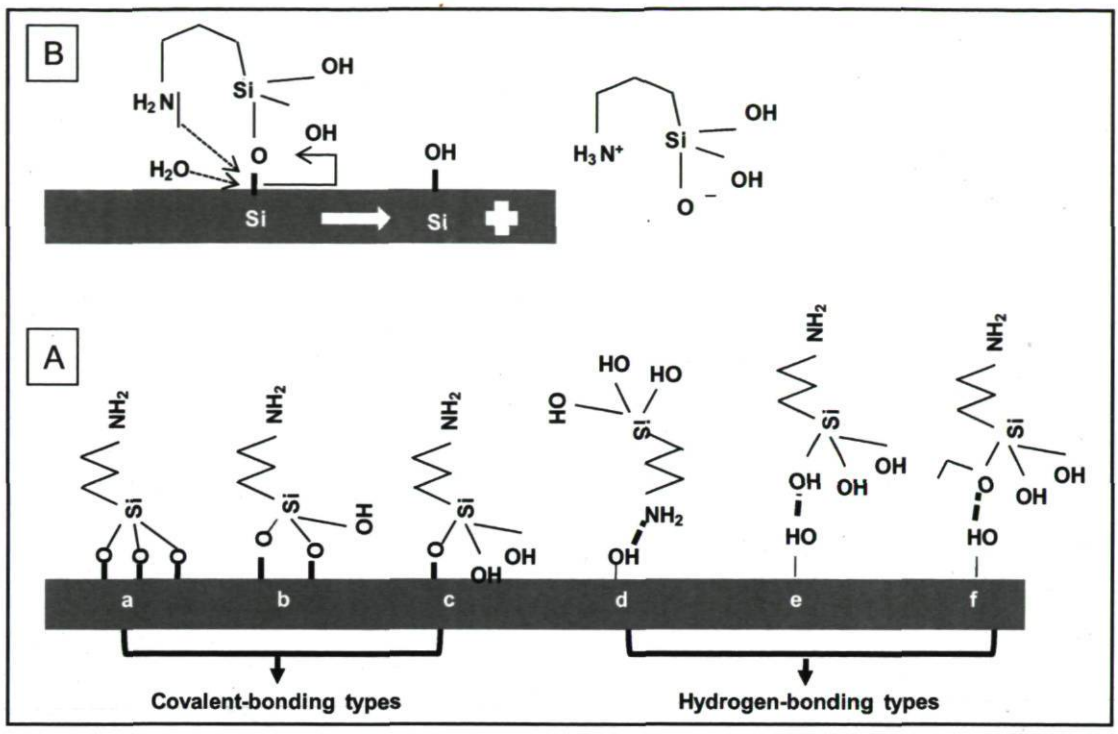

Figure S1. A) Different types of bonding/interaction between aminopropylethoxysilane molecules and silicon oxide substrates, B) Hydrolysis of siloxane bond,

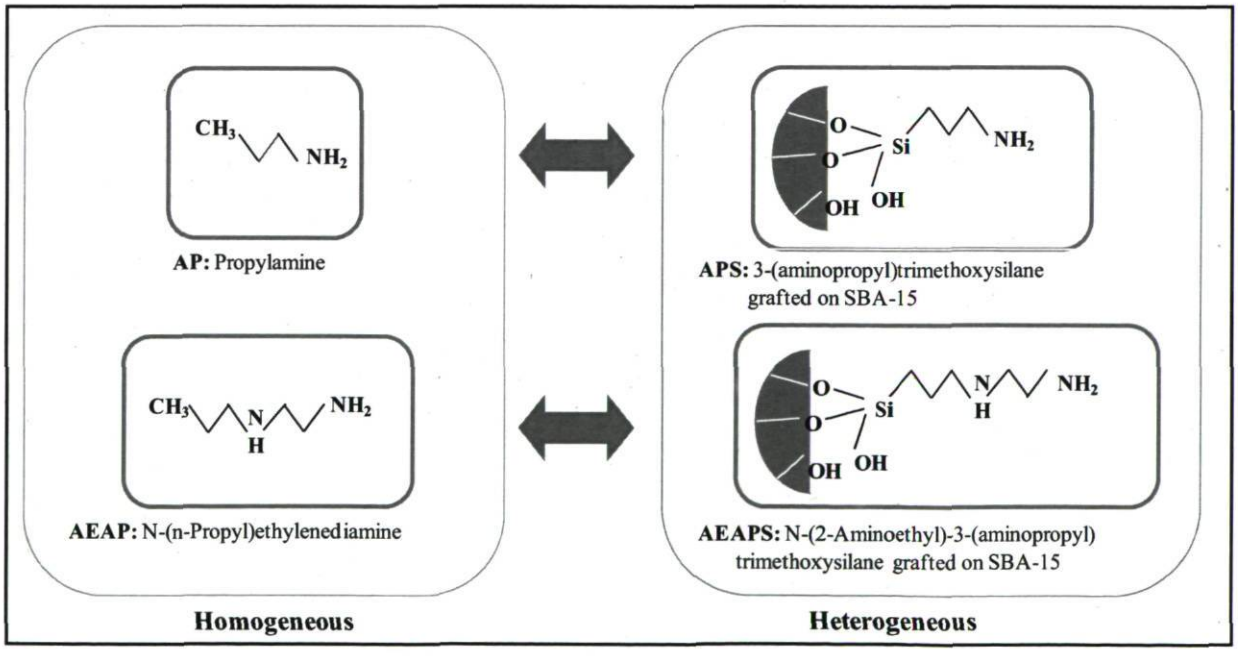

Figure S2. Schematic representation of grafted amines on SBA-15 (APS and AEAPS) and their equivalent non-grafted amines (AP and AEAP)

Table S1. Literature Summary of Grafted Amines on Mesoporous Silica Prepared Under Different Conditions Applied for CO_2 (Gas-Solid) Adsorption

		initial support/final product properties			grafting condition				adsorption condition			CO_2 adsorption capacity		CO_2 adsorption efficiency		
support material	amine type	BET S.A. (m^2/g)	pore di. (nm)	pore vol. (cm^3/g)	amino silane/ support[3] (cm^3/g)	H_2O/ alkoxy (mol/ mol)	t (°c)	amine content[4] (mmoln /g)	CO_2 partial pressure (kpa)	balance gas	t (°c)	dry CO_2 (mmol/g)	moist CO_2 (mmol/g)	dry CO_2 (CO_2/ N)	moist CO_2 (CO_2/ N)	ref.
HMS	APTMS	762/ 638	3/2.5	1.02/ 0.60	4	-	25	1.93	91	Ar	20	0.86	1.04	0.45	0.54	13
HMS	APTMS	1268/1194	2.4/ 2.0	0.98/ 0.62	3	-	25	1.64	91	Ar	20	0.87	-	0.53	-	13
HMS	APTMS	1198/1125	2.1/ 1.9	0.97/ 0.67	4	-	25	2.29	91	Ar	20	1.59	-	0.69	-	13
MCM-48	APTES	1389/-	-	-	5	-	70	2.3	5	He	25	1.14	2.3	0.50	1.00	11
MCM-48	APTES	1290/505	2.6/-	1.15/ 0.45	-	-	110	2.45	101	-	25	0.8	-	0.33	-	15
MCM-48	APTES	1290/5	2.6/-	1.15/0.1	-	1	110	3.99	101	-	25	0.1	-	0.03	-	15
MCM-41	APTES	1059/198	2.6/ 4.5	0.68/ 0.07	2.5	-	70	1.5	101	-	25	1.16	-	0.77	-	17
MCM-41	APTMS	1124/420	9.9/ 7.2	2.28/ 0.65	2	0.48	85	4.18	5	N_2	25	2.05	3.67	0.49	0.88	10
silica gel	APTMS	-/-	-/-	-/-	-	-	25	1.20	101	-	25	0.41	0.89	0.39	0.74	37
SBA-15	APTES	548/ 304	7.4/ 6.7	0.95/ 0.55	2.5	-	70	1.6	101	-	25	0.96	-	0.60	-	17
SBA-15	APTES	910/ 364	5.9/-	1.11/ 0.54	6	-	110	2.57	15	N_2	60	0.52	0.50	0.20	0.19	16
SBA-15	APTES	820/374	5.9/-	1.07/ 0.54	6	-	110	2.61	15	N_2	60	0.66	0.65	0.25	0.25	16
SBA-15	APTES	215/-	21/-	-	-	-	150		4	He		0.25	0.41	-	-	12
Xerogel	APTES	816/-	-	-	5	-	70	1.7	101	He	25	1.12	-	0.66	-	11

[3] per unit mass of initial support
[4] per unit mass of post-grafted support

HMS	AEAPTES	762/-	3/-	1.02/-	3.9	-	25	3.07	91	Ar	20	0.89	0.45	0.29	0.15	[14]
HMS	AEAPTES	1268/-	2.4/-	0.98/-	3	-	25	3.64	91	Ar	20	1.66	-	0.46		[14]
SBA-15	AEAPTMS	700/-	6.6/-	-/-	1	1.28	110	2.64	15	N_2	25	0.57	0.57	0.22	0.22	[38]
SBA-15	AEAPTMS	910/ 312	5.9/-	1.11/ 0.51	6	-	110	3.76	15	N_2	60	0.87	0.90	0.23	0.24	[16]
SBA-15	AEAPTMS	820/ 250	5.9/-	1.07/ 0.39	6	-	110	4.61	15	N_2	60	1.36	1.51	0.30	0.33	[16]
SBA-15	TA	910/ 240	5.9/-	1.11/0.4	8.5	-	110	4.85	15	N_2	60	1.1	1.21	0.23	0.25	[16]
MCM-41	TA1	1140/ -	3.7/-	1.03/-	3	-	85	5.95	5	N_2	25	1.08	1.18	0.18	0.20	[39]
MCM-41	TA1	950/ -	10/-	2.21/ -	3	0.48	85	7.98	5	N_2	25	2.65	2.94	0.33	0.37	[39]

1.6 References

(1) Morgan, M. G.; Keith, D. W. *Climate Change* **2008**, *90*, 189–215.

(2) Yamasaki, A. *J. Chem. Eng. Jpn.* **2003**, *36*, 361–375.

(3) Monastersky, R. *Nature* **2009**, *458*, 1091–1094.

(4) Hofmann, D. J.; Butler, J. H.; Tans, P. P. *Atmos. Environ.* **2009**, *43*, 2084–2086.

(5) Pennline, H. W.; Luebke, D. R.; Jones, K. L.; Myers, C. R.; Morsi, B. I.; Heintz, Y. J.; Ilconich, J. B. *Fuel Process. Technol.* **2008**, *89*, 897– 907.

(6) Chi, S.; Rochelle, G. T. *Ind. Eng. Chem. Res.* **2002**, *41*, 4178– 4186.

(7) Strazisar, B. R.; Anderson, R. R.; White, C. M. *Abs. Pap. Am. Chem. Soc.* **2002**, *223*, U569–U569.

(8) Nourouzi-Lavasani, S.; Larachi, F.; Benali, M. *Ind. Eng. Chem. Res.* **2008**, *47*, 7118–7129.

(9) Franchi, R.; Harlick, P. J.; Sayari, A. *Ind. Eng. Chem. Res.* **2005**, *44*, 8007–8013.

(10) Serna-Guerrero, R.; Da'na, E.; Sayari, A. *Ind. Eng. Chem. Res.* **2008**, *47*, 9406–9412.

(11) Huang, H. Y.; Yang, R. T.; Chinn, D.; Munson, C. L. *Ind. Eng. Chem. Res.* **2003**, *42*, 2427–2433.

(12) Chang, A.; Chuang, S. S.; Gray, M.; Soong, Y. *Energy Fuels* **2003**, *17*, 468–473.

(13) Knowles, G. P.; Graham, J. V.; Delaney, S. W.; Chaffee, A. L. *Fuel Process. Technol.* **2005a**, *86*, 1435–1448.

(14) Knowles, G. P.; Delaney, S. W.; Chaffee, A. L. *Nanoporous Mater. IV* **2005b**, *156*, 887–896.

(15) Kim, S.; Ida, J.; Guliants, V. V.; Lin, J. Y. *J. Phys. Chem. B* **2005**, *109*, 6287–6293.

(16) Hiyoshi, N.; Yogo, K.; Yashima, T. *Microporous Mesoporous Mater.* **2005**, *84*, 357–365.

(17) Zhao, H.; Hu, J.; Wang, J.; Zhou, L.; Liu, H. *Acta Physico-Chim. Sin.* **2007**, *23*, 801–806.

(18) Zhao, X. S.; Lu, G. Q. *J. Phys. Chem. B* **1998**, *102*, 1556–1561. (19) Jaroniec, C. P.; Kruk, M.; Jaroniec, M. *J. Phys. Chem. B* **1998**, *102*, 5503–5510.

(20) Goel, N. *J. Pet. Sci. Eng.* **2006**, *51*, 169–184.

(21) Chieh C. Fundamental characteristics of water. In *Handbook of food science, technology, and engineering*; Hui, Y. H., Culbertson, J. D., Duncan, S., Guerrero-Legarreta, I., Li-Chan, E. C. Y., Ma, C. Y., Manley, C. H., McMeekin, T. A., Nip, W. K., Nollet, L. M. L., Rahman, M. S., Toldra, F., Xiong, Y. L. CRC Press, Taylor and Francis: 2006; Vol. 1, Chapter 12, pp 12.1-12.17. Boca Raton, Florida, USA

(22) Cassiers, K.; Linssen, T.; Mathieu, M.; Benjelloun, M.; Schrijnemakers, K.; Van Der Voort, P.; Cool, P.; Vansant, E. F. *Chem. Mater.* **2002**, *14* (5), 2317–2324.

(23) Choi, M.; Heo, W.; Kleitz, F.; Ryong, R. *Chem. Commun.* **2003**, 1340–1341.

(24) Iliuta, M. C.; Larachi, F.; Grandjean, B. P. *Fluid Phase Equilib.* **2004**, *218*, 305–313.

(25) Le Tourneux, D.; Iliuta, I.; Iliuta, M. C.; Fradette, S.; Larachi, F. *Fluid Phase Equilib.* **2008**, *268*, 121–129.

(26) Asenath Smith, E.; Chen, W. *Langmuir* **2008**, *24*, 12405–12409.

(27) Etienne, M.; Goubert-Renaudin, S.; Rousselin, Y.; Marichal, C.; Denat, F.; Lebeau, B.; Walcarius, A. *Langmuir* **2009**, *25*, 3137–3145.

(28) Rosenholm, J. M.; Linde´n, M. *J. Controlled Release* **2008**, *128*, 157–164.

(29) Mokaya, R. *J. Phys. Chem. B* **1999**, *103*, 10204–10208.

(30) Khatri, R. A.; Chuang, S. S.; Soong, Y.; Gray, M. *Energy Fuels* **2006**, *20*, 1514–1520.

(31) Hicks, J.; Drese, J.; Fauth, D.; Gray, M. L.; Qi, G.; Jones, C. W. *J. Am. Chem. Soc.* **2008**, *130*, 2902–2903.

(32) Versteeg, G. F.; Van Swaaij, W. P. M. *J. Chem. Eng. Data* **1988**, *33*, 29–34.

(33) Mandal, B. P.; Kundu, M.; Bandyopadhyay, S. S. *J. Chem. Eng. Data* **2005**, *50*, 352–358.

(34) Al-Ghawas, H. A.; Hagewlesche, D. P.; Rulz-Ibanez, G. C.; Sandall, O. *J. Chem. Eng. Data* **1989**, *34*, 385–391.

(35) Saha, A. K.; Bandyopadhyay, S. S.; Biswas, A. K. *J. Chem. Eng. Data* **1993**, *38*, 78–82.

(36) Li, M.; Lai, M. *J. Chem. Eng. Data* **1995**, *40*, 486–492.

(37) Leal, O.; Bolivar, C.; Ovalles, C.; Garcia, J. J.; Espediel, Y. *Inorg. Chim. Acta* **1995**, *240*, 183-189.

(38) Zheng, F.; Tran, D. N.; Busche, B. J.; Fryxell, G. E.; Addleman, R. S.; Zemanian, T. S.; Aardahl, C. L. *Ind. Eng. Chem. Res.* **2005**, *44*, 3099-3105.

(39) Harlick, P. E.; Sayari, A. *Ind. Eng. Chem. Res.* **2007**, *46*, 446-458.

Conclusion and Recommendations

In spite of inherent corrosiveness and toxicity related to aqueous amine solutions, these have been the most traditional means for CO_2 capture in industry. In this study, by the aim of remedy to the problems of using aqueous amine, the effect of *liquid*-state water on CO_2 adsorption capacity of grafted amines on mesoporous materials was studied; SBA-15 functionalized with aminopropyltrimethoxysilane (APS) and N-(2-aminoethyl)-3-(aminopropyl)trimethoxysilane (AEAPS) were examined to evaluate the potential of this mode of contact in gas-liquid-solid scrubbing operations for CO_2 partial pressures range from 15 to 105 kPa. The results were compared to the CO_2 adsorption capacity of the grafted amines in moist and dry gas-solid conditions along with the CO_2 *absorption* capacity in gas-liquid amine solution systems consisting of amines with nearly identical structures.

Furthermore, hydrothermal stability of APS and AEAPS were examined by subjecting the samples to eight cycles of immersion tests in water at 40°C. The results revealed that maximum leaching occurred in the first two immersion cycles while the nitrogen content of AEAPS remains more or less stable after fourth immersion cycle, although a little instability was observed in almost all APS tests. Nitrogen sorption isotherms of C4-APS, C8-APS, C4-AEAPS and C8-AEAPS confirmed that the mesoporous structures of APS and AEAPS were retained during prolonged contact with liquid-state water.

Adsorption/ absorption result revealed that in equal amine concentrations, aqueous amines are more active than the ones grafted on mesoporous materials. In addition, at low CO_2 partial pressure, adsorption efficiency of C4-AEAPS in presence of liquid water surpassed the results obtained in presence of humid and dry CO_2 of gas-solid adsorption; while by increasing the CO_2 partial pressure the effect of physical adsorption in mesoporous structure which is most dominant in dry condition outperformed it over the result obtained in presence of moisture and liquid water. In heterogeneous conditions, the adsorption capacity of the C4-AEAPS (1.6 mmol N/g) varied within 300-413 μmol/g depending on CO_2 partial pressure.

Since the adsorption capacity of more than 1000 μmol/g is required for the reduction of CO_2 emission at large scale in an economic manner, [29] further increase in capacity is still necessary. Considering the low amine content of C4-AEAPS due to ~ 40 % leaching in contact with water, it is conceivable that modifying the amine groups with the purpose of controlling the leaching process and increasing the amine content, [30] could bring the CO_2 sorption capacity up to the level for an appeal for industrial applications. It also worth mentioning that according to this research, grafted amine adsorption efficiency is not considerably influenced by presence of liquid water compared to dry conditions in gas-solid adsorption, which represents a major advantage over adsorbents that even need stringent moisture control in their gas stream. Hence, it is conceivable that applying grafted amines inside the scrubber with slight water circulation could remedy the problems of using aqueous amine in conventional gas-liquid scrubbers.

Following the investigations described in this research, a number of factors associated with the heterogeneous process still require further investigations before practical application of CO_2 capture by grafted amine on mesoporous material can be envisaged. Some improvement routes could be:

- Grafting cyclam groups multiarms[27] to SBA-15 in order to restrict the amine degradation to a negligible extent;

- Based on the insight gathered on CO_2 adsorption capacity of grafted amines in heterogeneous conditions, using grafted cyclam groups in scrubbers with slight water circulation is expected to yield appealing capture performances as comparable as in homogeneous gas-liquid scrubbing.